Palaeontologia Electronica
palaeo-electronica.org

Fossil moles from the Gray Fossil Site (Tennessee): Implications for diversification and evolution of North American Talpidae

Danielle E. Oberg and Joshua X. Samuels

ABSTRACT

The Gray Fossil Site (GFS), an early Pliocene aged site in northeastern Tennessee, is one of the richest Cenozoic localities in the eastern United States. To date, thousands of micro-vertebrate specimens have been collected, but few small mammals have been identified and thoroughly studied. This study describes the first talpid specimens recovered from the GFS, which represent four talpid species *(Parascalops grayensis* sp. nov., *Neurotrichus* sp., *Mioscalops* sp., and a new stem desman, *Magnatalpa fumamons* gen. et sp. nov.).

The fossil taxa were quantitatively compared to a wide range of extant and extinct moles using a geometric morphometric analysis of humeri shape. Humeral morphology has commonly been used to diagnose talpid species and study their relationships. Quantitative analysis shows humerus shape is highly reflective of locomotor ecology in extant talpids, highlighting convergence among highly fossorial clades, and allows ecological inferences for fossil species. Hierarchical cluster analysis using morphometric data allowed examination of morphological similarity among taxa and helped to secondarily support taxonomic designations for the Gray Fossil Site taxa. The resulting phenogram shows strong similarity to the most up-to-date molecular cladogram and actually matched phylogenetic relationships substantially better than any morphological cladistic analyses to date. All six recognized tribes were represented on the cluster analysis phenograms, all of the shrew moles (Scaptonychini, Urotrichini, and Neurotrichini) clustered together, and there was some separation between the tribes Talpini and Scalopini. Additionally, the cluster analysis provides new information about the placement of fossil taxa and which parts of the tree still need better resolution.

Danielle E. Oberg. Department of Geosciences, University of Arkansas, Fayetteville, Arkansas 72701, USA. deoberg@uark.edu
Joshua X. Samuels. Department of Geosciences, East Tennessee State University, Johnson City, Tennessee 37614, USA. samuelsjx@mail.etsu.edu

Keywords: Talpidae; Gray Fossil Site; geometric morphometrics; systematics; paleoecology; new species

https://zoobank.org/204ACB38-BC8F-4DD6-9B4E-6A8B04517A17

Final citation: Oberg, Danielle E. and Samuels, Joshua X. 2022. Fossil moles from the Gray Fossil Site, Tennessee: Implications for diversification and evolution of North American Talpidae. Palaeontologia Electronica, 25(3):a33. https://doi.org/10.26879/1150
palaeo-electronica.org/content/2022/3718-moles-from-gray-fossil-site

Submission: 6 January 2021. Acceptance: 5 November 2022.

INTRODUCTION

Talpidae (true moles, shrew moles, and desmans) is an ecologically diverse family that is widely distributed across the northern hemisphere (Nowak and Paradiso, 1983; Gorman and Stone, 1990; Gunnell et al., 2008). Talpids are well known for their subterranean lifestyles and unique morphological modifications for fossorial specialization (Freeman, 1886; Campbell, 1939; Reed, 1951; Yalden, 1966; Hildebrand, 1985; Gorman and Stone, 1990; Sánchez-Villagra et al., 2004; Meier et al., 2013); however, semi-aquatic and terrestrial locomotor ecologies are also common (Nowak and Paradiso, 1983; Gorman and Stone, 1990). Even though there are variable locomotor ecologies among extant talpids, convergent evolution can strongly influence body shape, creating problems for researchers interested in understanding the evolutionary history and diversification of the family.

Convergent evolution among specialized clades has created major discrepancies between talpid molecular and morphological phylogenies (Douady et al., 2002; Symonds, 2005; Sánchez-Villagra et al., 2006; He et al., 2016). Similar morphology among clades makes it difficult to choose morphological characters independent of ecology, and most molecular studies also lack confidence on cluster positions. Previous studies (Rohlf et al., 1996; Piras et al., 2012; Sansalone et al., 2015) have shown that geometric morphometrics can be useful for assessing relationships in talpids.

The fossil record for Talpidae is somewhat known; the oldest members of the family are from the Eocene of Europe (Hooker, 2016) and peak diversity occurred during the Miocene of both Eurasia and North America (Gunnell et al., 2008). Though talpids in North America are discussed by Gunnell et al. (2008), there has yet to be a detailed review of the family, and thus, relatively little is known about the diversification of, and relationships between, North American talpid species. We describe new talpid occurrences from the Gray Fossil Site, which help to fill gaps in the North American fossil record, reveal dispersal patterns between Eurasia and North America, and can improve understanding of talpid evolution during the Cenozoic.

The new moles from the Gray Fossil Site, and a wide range of modern and fossil moles, are quantitatively analyzed here using 2D geometric morphometric analyses of the humerus. These analyses can highlight how morphology reflects locomotor ecology of talpids, facilitate paleoecological inferences for extinct species, and reveal morphological similarity among taxa that can support qualitative inferences of their relationships. These analyses may improve understanding of the source of discrepancies between molecular and morphological phylogeneties, and hold potential to reveal potentially phylogenetically informative morphological features.

Background

Talpidae is an ecologically diverse family consisting of: terrestrial shrew moles, semi-fossorial shrew moles, semi-aquatic desmans, as well as semi-fossorial and fossorial moles (Koyabu et al., 2011). Currently, the most parsimonious phylogenetic hypothesis comes from He et al. (2016). There are three subfamilies within Talpidae: Uropsilinae (Asian shrew-like moles), Talpinae (Old World moles, desmans, and shrew moles), and Scalopinae (New World moles), and there are seven tribes: Scalopini (North American/Asian fossorial moles), Scaptonychini (Chinese fossorial long-tailed moles), Urotrichini (Japanese semi-fossorial shrew moles), Neurotrichini (North American semi-fossorial shrew moles), Condylurini (North American semi-fossorial star-nosed mole), Desmanini (Eurasian semi-aquatic desmans), and Talpini (Eurasian fossorial moles). Though the Scaptonychini tribe does not contain any shrew moles, it is most similar both molecularly and morphologically to the extant shrew mole groups. Two of the six clusters are exclusively fossorial: the Eurasian Talpini and North American/Asian Scalopini. It is hypothesized that these two clusters convergently evolved similar derived morphological specializations for fossorial life (Gorman and Stone, 1990; Piras et al., 2012; Meier et al., 2013; He et al., 2016).

Ancestors to talpids are hypothesized to have been fully terrestrial. Sometime before or during the Eocene, there would have been a transformation from a terrestrial to a fossorial life style (Sánchez-Villagra et al., 2004), which resulted in the humerus of fossorial moles becoming extremely broad, and compact, with pronounced muscle attachments (Yalden, 1966; Hildebrand, 1974;

Whidden, 2000; Gambaryan et al., 2002; Meier et al., 2013). Additionally, both proximal and distal ends are positioned in opposite directions, which relates to mid-shaft torsion (Freeman, 1886; Whidden, 2000). This humeral morphology is only found in talpids (Reed, 1951; Yalden, 1966; Sánchez-Villagra et al., 2004; Meier et al., 2013), and several studies (Gambaryan et al., 2002; Meier et al., 2013) have shown this morphology is most likely related to the expansion of muscle attachment sites.

Forelimb robustness increases the likelihood of humeri being preserved but can also provide insights into locomotor adaptations through time. However, the resolution of locomotor adaptations through time requires a well-resolved phylogeny. Numerous phylogenetic hypotheses have been proposed based on osteological, myological, and molecular data (Hutchison, 1976; Yates and Moore, 1990; Whidden, 2000; Motokawa, 2004; Shinohara et al., 2004; Cabria et al., 2006; Sánchez-Villagra et al., 2006; Bannikova et al., 2015; Schwermann and Thompson, 2015; Sansalone et al., 2018; 2019, 2020; Schwermann et al., 2019), but often they reveal more conflicts rather than resolve the problem. This creates additional problems regarding the establishment and composition of subfamilies and tribes (Hutchison, 1968; Yates, 1984; McKenna and Bell, 1997; Hutterer, 2005), with substantial confusion surrounding the phylogenetic placement and taxonomic assignment of fossil forms (Ziegler, 2003; 2012; Klietmann et al., 2015; He et al., 2016; Sansalone et al., 2018). Recent work by He et al. (2016) has produced a molecular based phylogeny with strong statistical support for each clade. We are using this phylogeny as the comparative phylogeny for the remainder of this study.

Geologic Setting

The Gray Fossil Site (GFS) is an early Pliocene, latest Hemphillian or earliest Blancan North American Land Mammal Age (NALMA), site in northeastern Tennessee. Age of the GFS is inferred to be between 4.9 and 4.5 Ma, based on the presence and biostratigraphic ranges of the rhino *Teleoceras*, the cricetids *Neotoma* and *Symmetrodontomys*, and the leporid *Notolagus lepusculus* (Samuels et al., 2018; Samuels and Schap, 2021). The geology includes multiple karst subbasins that filled with lacustrine sediments (Shunk et al., 2006; Whitelaw et al., 2008; Shunk et al., 2009), which indicates that the GFS was once a limestone paleosinkhole that filled in and became a 40 m-deep paleosinkhole lake (Shunk et al., 2006, 2009; Zobaa et al., 2011). The stratigraphy consists of thin layers of locally derived silts and sands with low organic content overlain by thin layers of organic matter with alternating bands of quartz sand and carbonate silt (Shunk et al., 2006, 2009).

Numerous vertebrate taxa and abundant plant fossils (e.g., Wallace and Wang, 2004; Liu and Jacques, 2010; Boardman and Schubert, 2011; Worobiec et al., 2013; Zobaa et al., 2011; Mead et al., 2012; Ochoa et al., 2012, 2016; Bourque and Schubert, 2015; Czaplewski, 2017; Jasinski and Moscato, 2017; Doughty et al., 2018; Jasinski, 2018; Samuels et al., 2018; Short et al., 2019; Quirk and Hermsen, 2020; Siegert and Hermsen, 2020) indicate that there was a dense forest surrounding the paleosinkhole lake. The lake was a year-round water source that supported the presence of fish, neotenic salamanders, aquatic turtles, alligators, and beavers (Parmalee et al., 2002; Boardman and Schubert, 2011; Mead et al., 2012; Jasinski, 2018; Bourque and Schubert, 2015). The plants suggest that the flora was predominantly oak, hickory, and pine forest (Ochoa et al. 2016), which resembles what is currently found in lower elevations of the southern Appalachians (Wallace and Wang, 2004; Gong et al., 2010). The flora also indicates strong Asian influences (Gong et al., 2010; Liu and Jacques, 2010; Ochoa et al., 2012; Quirk and Hermsen, 2020), and the presence of humid, wetland areas (Brandon, 2013; Worobiec et al., 2013). Carbon and oxygen isotopic analyses from GFS ungulate teeth suggest a dense forest around the lake and climate with little seasonal temperature and precipitation variation (DeSantis and Wallace, 2008).

METHODS

Morphological comparisons of extant and extinct talpid taxa, supplemented with linear measurements, were used to determine taxonomic identifications for the Gray Fossil Site talpid material. We examined dental material (n=152 maxillae and n=69 mandibles) and postcrania (n=135 humeri) from all 17 extant talpid genera (*Condylura* n=19, *Desmana* n=2, *Dymecodon* n=2, *Euroscaptor* n=3, *Galemys* n=3, *Mogera* n=3, *Neurotrichus* n=15, *Parascalops* n=10, *Parascaptor* n=1, *Scalopus* n=25, *Scapanulus* n=3, *Scapanus* n=13, *Scaptochirus* n=2, *Scaptonyx* n=3, *Talpa* n=3, *Uropsilus* n=6, and *Urotrichus* n=2), along with skeletal material for 21 extinct species for morphological comparisons. We did not examine any postcranial material for *Desmana* or *Parascaptor*. Extant mate-

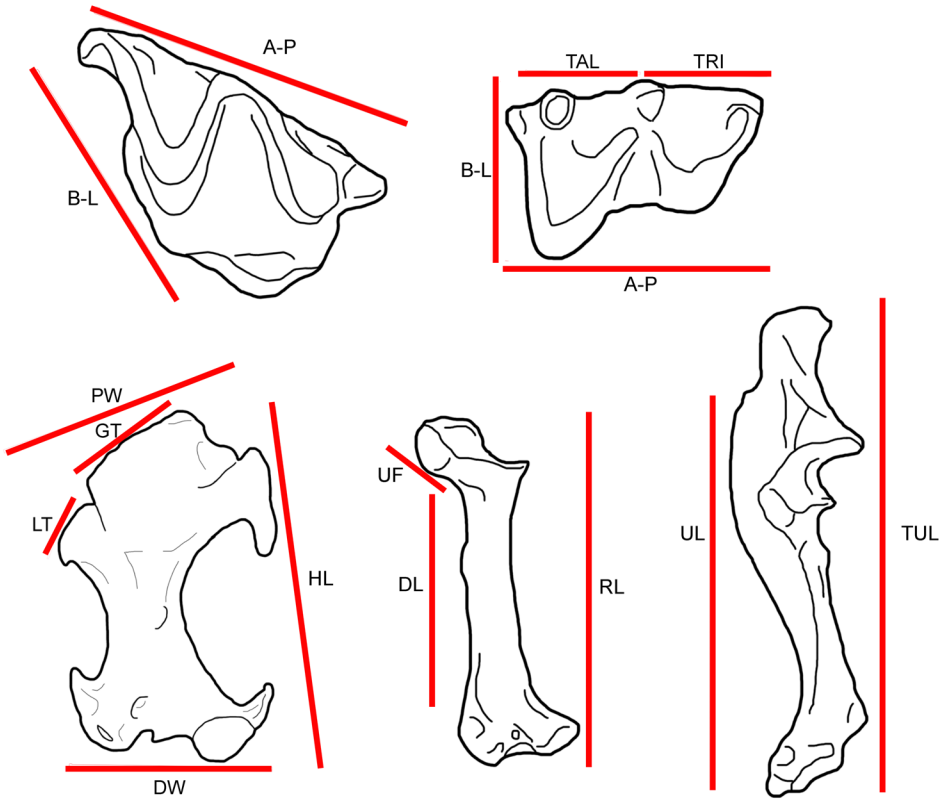

FIGURE 1. Linear measurements used for morphological comparison. B-L - buccolingual width; upper teeth - posterior-most tip of the metastyle to the lingual margin of the protocone; lower teeth - lingual-most tip of the metaconid to the buccal margin of the talonid. A-P - anteroposterior length; upper teeth - posterior-most tip of the metastyle to the anterior-most tip of the parastyle; lower teeth - anterior tip of the trigonid (paraconid) to the posterior end of the talonid (entostylid). TRI - width of the trigonid. TAL - width of the taloned basin. HL - total humerus length; proximal-most tip of greater tuberosity to distal-most point on capitulum. PW - width of the proximal end of the humerus: lateral most extent of the lesser tuberosity to the medial most aspect of the greater tuberosity. GT - length of the greater tuberosity. LT - length of the lesser tuberosity. DW - width of the distal end of the humerus: lateral most extent (entepicondylar process) to the medial most extent (ectepicondylar process). RL - total radius length: proximal-most tip of capitular process to distal-most tip of lunar articular facet. DL - length of the diaphysis. UF - length of the lunar articular facet. TUL - total ulna length; proximal-most tip of olecranon process to distal-most tip of terminal process. UL - ulna length without the olecranon fossa. Elements not to scale.

rial came from the Smithsonian Institution - National Museum of Natural History (USNM), Natural History Museum of Los Angeles County (LACM), the East Tennessee State University comparative osteology collection (ETMNH), and published literature sources. Fossil material came from published literature and the East Tennessee State University Museum of Natural History (ETMNH).

Extant specimens were photographed in standard diagnostic views (dental: lingual, labial, and occlusal; postcrania: anterior, posterior, and lateral). All material was photographed using either a Canon Rebel Ti DSLR camera with a macro lens attached to a copy stand or a Dino-Lite Edge AM4815ZT digital microscope camera using the associated DinoCapture 2.0 software version 1.5.27.A. Linear measurements (Figure 1) were taken on specimens using Fisher Scientific Traceable Digital Calipers 0-150 mm and photographs analyzed in ImageJ (Schneider et al., 2012).

We performed a 2D geometric morphometric analysis by digitizing 24 landmarks onto 135 humeri (*Condylura* n=16, *Dymecodon* n=1, *Euroscaptor* n=3, *Galemys* n=3, *Mogera* n=3, *Neurotrichus* n=15, *Parascalops* n=6, *Scalopus* n=22, *Scapanulus* n=1, *Scapanus* n=13, *Scaptochirus* n=2, *Scaptonyx* n=1, *Talpa* n=3, *Uropsilus* n=6, *Urotrichus* n=1, and fossils n=27), representing 42

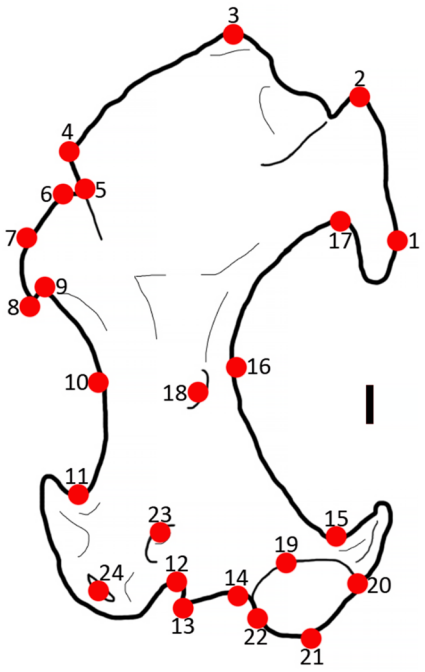

FIGURE 2. Number and position of humerus landmarks. Line drawing showing landmarks positions with labels on the anterior view of a left humerus of *Condylura cristata* (Star-nosed mole). Scale bar equals 1 mm.

taxa. We used the TPS Software series to do the geometric morphometrics analyses (Rohlf, 2006). Landmarks (Figure 2, Table 1) were chosen, and modified, from previous studies (Piras et al., 2012; Sansalone et al., 2015). Only one view (anterior) was used allowing us to maximize the number of taxa that could be included in the analysis.

We performed a relative warps analysis (RWA) using the tpsRelw program, to examine variation in humerus shape among taxa. As part of the RWA, landmark data were scaled, rotated, and aligned via Generalized Procrustes Analysis. Partial warp scores, uniform components, and relative warp scores derived from RWA were saved for subsequent analyses in SPSS 24 (IBM Corp., 2013). While not inherently biologically meaningful, partial warp scores can be used for multivariate statistical analyses that reveal biologically meaningful information (Adams et al., 2004; Webster and Sheets, 2010; Mitteroecker and Bookstein, 2011; MacCleod, 2017). We ran a canonical variates analysis (CVA) in SPSS using partial warp scores and uniform components to examine how humeral morphology of moles was related to locomotor ecology and to classify the paleoecology of extinct moles. Partial warp scores were used because they reflect the spatial information supplied by the reference shape, meaning they can be

TABLE 1. Numbers and Descriptions of All Landmarks. Directionality of character naming reflects orientation in Figure 3. Characters labeled and named according to Hutchison (1968).

Landmark	Description
1	Distal end of lesser tuberosity
2	Proximal end of lesser tuberosity
3	Proximal end of greater tuberosity
4	Distal end of greater tuberosity
5	Inflection between greater tuberosity and teres tubercle
6	Proximal end of teres tubercle
7	Greatest point of curvature on teres tubercle
8	Distal end of teres tubercle
9	Inflection between teres tubercle and minor sulcus
10	Greatest point of curvature of minor sulcus
11	Inflection between minor sulcus and entepicondylar process
12	Inflection between *M. flexor digitorum* ligament and trochlea
13	Lateral aspect of trochlea
14	Medial aspect of trochlea
15	Inflection between capitulum and major sulcus
16	Greatest point of curvature of major sulcus
17	Inflection between major sulcus and greater tubercle
18	Pectoral tubercle
19	Superior aspect of capitulum
20	Medial aspect of capitulum
21	Inferior aspect of capitulum
22	Lateral aspect of capitulum
23	Entepicondylar foramen
24	Fossa of the *M. flexor digitorum* ligament

used as a geometric reference system that is completely independent of any sample, but they must be tied to a standard convention (in this case, sample mean). The uniform components were used because they describe overall changes in proportions, typically in a linear fashion. Locomotor ecologies (Table 2) were derived from literature sources and all extant taxa were categorized into one of four groups. Locomotor classification of extant taxa was based on published physical observations of movement. Fossil taxa were included as unknowns to be classified by the analysis. While several recent studies (Mitteroecker and Bookstein, 2011; Cardini et al., 2019; Rohlf, 2021) have pointed to problems with using CVA in studies with high-dimension data (like many geometric morphometric analyses), our analysis includes a far greater

TABLE 2. Defining Locomotor Categories. Locomotor categories used in this study and their definitions were modified from Polly (2007).

Locomotor category	Description
Terrestrial	Spends most of time foraging on ground. May maintain a burrow for sleeping.
Semi-aquatic	Spends most of time foraging in water. May maintain a burrow for sleeping.
Semi-fossorial	Spends time foraging underground and on the surface.
Fossorial	Fully subterranean lifestyle.

number of sampled specimens (=135 humeri) than variables (48 partial warps and 2 uniform components), meaning our analysis does not inherently display data dimensionality bias.

A hierarchical cluster analysis, using the UPGMA clustering method with squared Euclidian distance, was conducted using partial warp scores and uniform components as variables. The cluster analysis was used to examine morphological similarity of taxa, while attempting to exclude features that were linked to locomotor ecology. Our goal was to examine similarity of taxa beyond morphological adaptations for digging, which are widely recognized and documented as being at least partially a consequence of convergence in Talpidae. Variables in the CVA of locomotor groups with a correlation coefficient greater than 0.3 were considered functionally-linked and excluded from the cluster analysis. The cluster analysis results were input into Mesquite (Maddison and Maddison, 2018) to visualize change in continuous and categorical variables across the dendrogram.

Two cluster analysis dendrograms were generated: one using all individuals and the other using species means. The dendrogram depicting individuals was used to see how well pre-existing clusters could be recreated. The species means dendrogram shows the average position for each taxon and was used for comparison against the most up-to-date molecular phylogeny by He et al. (2016) to evaluate goodness-of-fit.

Finally, we examined global talpid dispersion patterns through the Cenozoic using occurrence data from the NOW database (https://nowdatabase.org/), NEOTOMA databases (FAUNMAP and MIOMAP (Carrasco et al., 2007; Graham and Lundelius, 2010; http://www.ucmp.berkeley.edu/neomap/)), and a variety of literature sources. Maps were created in QGIS version 2.18.

SYSTEMATIC PALEONTOLOGY

Class MAMMALIA Linnaeus, 1758
Order SORICIMORPHA Gregory, 1910
Family TALPIDAE Fischer von Waldheim, 1814
Subfamily TALPINAE Fischer von Waldheim, 1814
Tribe ?DESMANINI Thomas, 1912
Genus *MAGNATALPA* gen. nov.

zoobank.org/0CC5C6F2-812B-4D4A-AF11-AAA8D37AB48E

Magnatalpa fumamons sp. nov.
Figure 3A - J

zoobank.org/9A3A7163-408A-4159-857B-A0AAA50D56A0

Type material. ETMNH 9664 - right m2.
Paratypes. ETMNH 20747 - left M1; ETMNH 20779 - right M1; ETMNH 21077 - right partial edentulous dentary.
Type locality. Gray Fossil Site, TN, USA.
Etymology. Genus *Magnatalpa* translates into large mole, as this dental material represents a mole that was much larger than all North American extant moles, fossil moles and desmans, and comparable in size to extant desmans (Table 3). The species is named *M. fumamons* due to the material's proximity to the Smoky Mountains.
Diagnosis. Large size; anteroposteriorly elongated lower molar; m2 lacking anterior, posterior, and lingual cingulids; m2 cristid obliqua joins metaconid; upper molars with continuous mesostyle; M1 lingual border with distinct, lingually projecting, protoconule and metaconule, either larger than or equal in size to the protocone.
Differential diagnosis. *Magnatalpa fumamons* lacks a divided mesostyle on the M1, a character unique to all true and extant desmans. *Magnatalpa fumamons* m2 lacks an anterolabial cingulum and a small cuspule on the cingulum in the re-entrant valley, differentiating it from all nine species of *Archaeodesmana*. *Magnatalpa fumamons* m2 has similarly sized trigonid and talonid as well as separate metaconid and entoconid, differentiating it from all species of *Asthenoscapter*. *Magnatalpa fumamons* m2 has a cristid obliqua that joins at the metaconid and has a large re-entrechat valley, differentiating it from all species of *Mygalea. Magnatalpa fumamons* teeth are substantially larger than those of *Mygalinia hungarica* (Table 3). *Magnatalpa fumamons* m2 has a wider re-entrechat valley than all fossil species of *Desmana*.

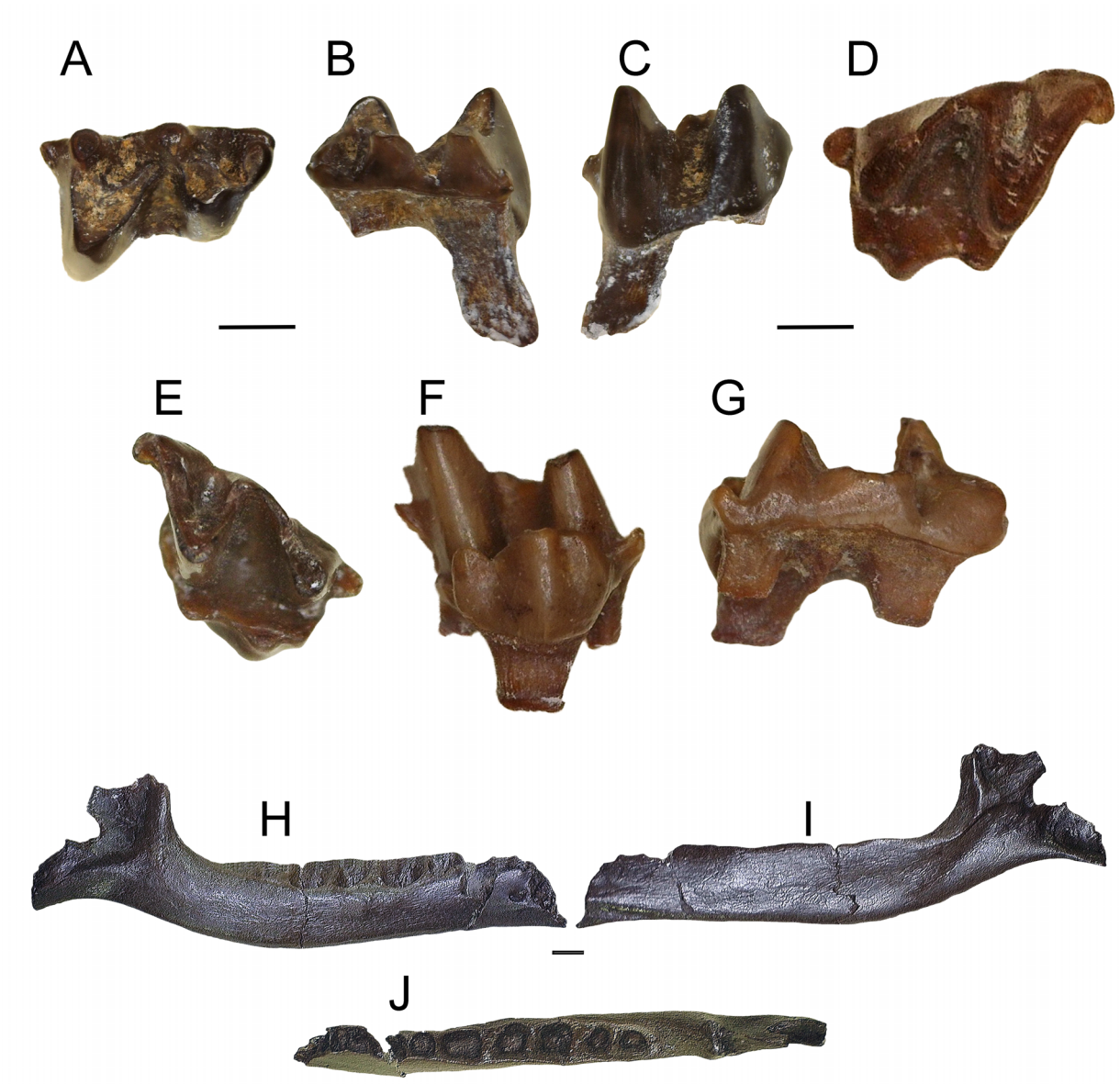

FIGURE 3. *Magnatalpa fumamons* gen. et sp. nov. dental material. ETMNH 9664, right m2 - A) occlusal, B) labial, and C) lingual views. ETMNH 20747, left M1 - D) occlusal view. ETMNH 20779, right M1 - E) occlusal, F) lingual, and G) labial views. ETMNH 21077, edentulous dentary - H) lingual, I) labial, and J) occlusal views. Scale bars equal 1 mm.

Description. The holotype m2, ETMNH 9664, is a very large tooth for a talpid (Figure 3A - C, Table 3). The cusps are relatively worn. The talonid is about the same length as the trigonid, but substantially wider. The entire tooth is anterioposteriorly elongate. The talonid and trigonid are both very open. There is a large reentrant valley between the trigonid and talonid. The cristid obliqua joins with the metaconid. There are no anterior, posterior, or lingual cingulids. The paraconid, metaconid, and entoconid are much lower than protoconid and hypoconid. The metaconid and entoconid are about the same size, but the metaconid is a little larger. The entoconid shows signs of heavy wear. The entostylid is large and triangular. The paraconid has an extra bladed notch along the posterior aspect.

ETMNH 20747 and 20779 both resemble a typical talpid M1, but are large (Figure 3D - G, Table 3). They have a lopsided triangular outline

TABLE 3. Desman Tooth Size Comparisons with *Magnatalpa fumamons* gen. et sp. nov.material. A-P is anteroposterior length. B-L is buccolingual width. Measurements in mm. Min-max ranges provided for those with multiple samples. The ranges for *Archaeodesmana* include all 9 accepted species (*A. pontica*, *A. vinea*, *A. turolensis*, *A. adroveri*, *A. luteyni*, *A. major*, *A. dekkersi*, *A. brailloni* and *A. bifida*). The ranges for *Desmana* includes five accepted fossil species (*D. kowalskae*, *D. nehringi*, *D. inflata*, *D. thermalis*, and *D. marci*).

Taxon	M1		m2	
	A-P	B-L	A-P	B-L
Desmana moschata (n = 8)	2.95 - 4.60	2.55 - 4.70	2.25 - 4.00	3.00 - 3.32 (n = 3)
Desmana (Minwer-Barakat et al., 2020)	2.20 - 2.90	--	2.50 - 3.40	--
Galemys pyrenaicus (n = 12)	2.35 - 3.30	2.20 - 3.39	2.20 - 2.95	1.18 - 2.11 (n = 8)
Mygalinia hungarica (Rzebik-Kowalska and Rekovets, 2016)	--	--	2.00 - 2.10 (n = 4)	1.30 - 1.40 (n = 4)
Mygalea magna (van den Hoek Ostende and Fejfar, 2016)	1.77 - 2.05 (n = 8)	1.94 - 2.19 (n = 8)	1.87 - 2.26 (n = 60)	1.23 - 1.29 (n = 60)
Archaeodesmana (Martín-Suárez et al., 2001)	2.60 - 3.50	2.00 - 3.10	2.10 - 2.70	--
Lemoynea biradicularis (Bown, 1980)	2.71 - 2.72	2.92 - 3.08	2.17 - 2.28	1.56 - 1.75
ETMNH 20747	3.41	3.35	-	-
ETMNH 20779	3.57	3.43	-	-
ETMNH 9664	-	-	2.98	2.37

due to the great difference in the morphology of the labial cusps and have pre- and post-cingula. The paracone and metacone are crescentic in shape and relatively similar in size, but the paracone is slightly smaller. The protocone is also large and centrally placed. The teeth are very open; the paracone and metacone are well separated. There is a large paraconule about the same size as the paracone. The mesostyle is not divided. The protoconule and the metaconule are well developed and influence the lingual outline of the crown causing the antero- and posterolingual side to bulge outwards. The protoconule is closely appressed to the anterior margin of the protocone. A deep basin lies between the protocone, paracone, and metacone.

ETMNH 21077 is a partial right edentulous dentary. The dentary is broken at the fourth antemolar. There are alveoli for four antemolars, m1, m2, and m3 (Figure 3H - J). There are two alveoli per molar for two roots. The alveoli for m2 are the largest, while m3 are the smallest. Each antemolar has only one alveolus and they decrease in size anteriorly. The total length of the partial dentary is 17.46 mm, and it is 2.68 mm deep at the m2 anterior alveolus. The ascending ramus and mandibular angle are broken off, but a portion of the masseteric fossa is preserved.

Discussion. The formal systematic classification of desmans has been debated for quite some time. This group was previously classified as a subfamily (Barabasch-Nikiforow, 1975; Hutchison, 1974; Rümke, 1985) called Desmaninae. Some researchers thought there was enough morphological distinction between desmans and other talpids to warrant a family-level designation; however, recent genetic work (Shinohara et al., 2003; Shinohara et al., 2004; He et al., 2014, 2016) shows that this group falls within the subfamily Talpinae and should be classified as a tribe.

The morphology and size of these three molars are reminiscent of extant desmans, but these teeth do not represent either of the two extant genera. The GFS specimens are comparable in size to *Desmana moschata* (Russian desman) but are larger than *Galemys pyrenaicus* (Pyrenees desman) (Table 3). The M1 of extant desmans resembles that of other talpids in occlusal shape and generalized morphology. However, extant desman upper molars always have a divided mesostyle (also referred to as distinctly twinned mesostyle) and a strongly developed lingual part featuring a protoconule, a protocone, a metaconule and often a small tubercle on the posterocrista of the protocone (Miller, 1912; Schreuder, 1940; Hugueney, 1972; Rümke, 1985). These cuspules act like additional cusps and increase the food processing surface area on the tooth, aiding in efficient food processing (Rümke, 1985).

An important feature that has been used as an apomorphy for defining the tribe Desmanini is the cristid obliqua of the lower molars ends either 1) against the tip of the metaconid, or 2) against the protoconid-metaconid crest (Miller, 1912; Schreuder, 1940; Hugueney, 1972; Rümke, 1985). Specifically looking at the m2, a strong entostylid is always present in extant desmans. It can be either a bulge formed by the posterior cingulum or a rounded or elliptical tubercle situated near the enamel-dentine boundary. The shape and size of the cusps, as well as the position of cristid obliqua are highly variable. The teeth can be heavy with sturdy obtuse cusps and high connecting ridges, or more slender with sharp cusps and low crests. The cristid obliqua may be short or long, ending either against the protoconid-metaconid crest or near the tip of the metaconid (Rümke, 1985).

The teeth of extant desmans are most morphologically similar to extant shrew moles, but are larger (Schreuder, 1940; Rümke, 1985). In lower molars, the talonid is v-shaped like all talpids, not u-shaped like soricids. In the upper molars, accessory cuspules along the lingual boarder in desmans' functions like the hypocone in shrew moles (Schreuder, 1940; Hutchison, 1974; Palmeirim and Hoffmann, 1983; Carraway and Verts, 1991). The cusps on upper and lower molars tend to be brachydont, when compared to other extant talpids, and more bulbous because the diet of extant desmans consists of benthic invertebrates (Palmeirim and Hoffmann, 1983; Rümke, 1985).

The two isolated upper teeth from GFS share characteristics of both *Lemoynea* and *Mystipterus*. *Lemoynea* is a basal desmanine talpid known from the early late Miocene (Clarendonian) of Nebraska (Bown, 1980), which is the oldest confirmed desman in North America. The molars of *Lemoynea* are reminiscent of extant desmans: they are relatively large in size (Table 3), all three upper molars have a divided mesostyle, and there are lingual cuspules on the occlusal surface of the upper molars (Brown, 1980; Gunnell et al., 2008). The GFS teeth look very much like the teeth of *Lemoynea,* but they lack the divided mesostyle, which is considered a derived feature of the tribe. *Mystipterus* is a basal talpid (Uropsilinae) known from the late Oligocene to late Miocene (Arikareean to Clarendonian) of the Great Plains and Oregon (Gunnell et al., 2008). It looks more shrew-like than other talpids: there is a large hypocone flaring off the posterior aspect of the upper molars, it does not have a divided mesostyle, and it does not have accessory lingual cuspules on the occlusal surface (Hutchison, 1968). The GFS teeth have the continuous mesostyle like *Mystipterus* and other basal talpids but lack the same generalized occlusal morphology and presence of a hypocone.

The GFS teeth are distinct from European fossil desman genera: *Asthenoscapter*, *Mygalea*, *Mygalinia*, and *Desmana*. *Asthenoscapter* detention is morphologically more similar to Uropsilinae, especially *Mystipterus*, than other ?Desmanini (Hutchison, 1968; 1974). The molars of *Asthenoscapter* are nearly morphologically identical to *Mystipterus* in proportion, cingulid development, relative cuspid size, and cristid arrangement. The m2s of *Asthenoscapter* species have a narrower trigonid than talonid and a very well-developed metacristid, which is continuous with the entocristid (Hutchinson, 1974), whereas *M. fumamons* has similarly sized trigonid and talonid as well as a separate metaconid and entoconid. *Mygalea* m2s have a cristid obliqua is directed towards the middle of the protocnid-metaconid crest but bends sharply and ends at the metaconid or metacristid and a small re-entrechat valley (Van den Hoek Ostende and Fejfar, 2006), whereas *M. fumamons* has a cristid obliqua that joins at the metaconid and has a large re-entrechat valley. *Mygalinia* m2 trigonid and talonid are more or less of the same size, the oblique cristid reaches the tip of the metaconid and the re-entrant valley is deep (Rzebik-Kowalska and Rekovets, 2016), which is morphologically similar to *M. fumamons*; however, *Mygalinia* was a substantially smaller desman based on tooth size (Table 3). Fossil species of *Desmana* m2s are typical for desmans with heavy and have sturdy obtuse cusps, cristid obliquids are long and end near the tip of the metaconid (Topachevsky, 1962). Cingulids are wide and present on anterior, buccal, and posterior sides. Unlike *M. fumamons*, the re-entrant valley is narrow in all fossil species of *Desmana*.

All three GFS teeth are distinct from the well-known fossil desman, *Archaeodesmana*. *Archaeodesmana* is known from the late Miocene to early Pliocene of Europe (Hutterer, 1995, Minwer-Barakat et al., 2020). The M1 of *Archaeodesmana* is morphologically similar to the extant species *Galemys pyrenaicus*, with a poorly developed metastyle and a divided mesostyle. On all three lower molars, the anterolabial cingulum is well developed, and sometimes there is a small cuspule on the cingulum in the re-entrant valley (Martín-Suárez et al., 2001). These characteristics are not present on any of the GFS specimens, thus excluding *Archaeodesmana*.

The GFS partial dentary is also morphologically distinct from other known desmans. In specimens identified as *Lemoynea*, the ventral border of the horizontal ramus becomes deeply inflected posteriorly beneath the m1 hypoflexid and anteriorly beneath the anterior root of p3 (Brown, 1980). The dentary is deepest beneath m2 in *Desmana moschata*, *Galemys pyrenaicus*, and all known species of *Archaeodesmana* (Brown, 1980; Ziegler, 2005). The GFS dentary has no inflections, nor does it deepen; the body of the dentary is smooth and continuous. Specimens of *Lemoynea* possess a large mental mandibular foramen situated beneath the posterior root of m1, about one-third the distance from the inferior border of the mandible to the alveolar border of the tooth row (Brown, 1980). In *Archaeodesmana* species, there are two mental foramina: the anterior one under the p1 or below p1/p2, and the posterior one under the trigonid of m1 or below the posterior root of p4 (Ziegler, 2005). In fossil *Desmana* species, tri- or quadripartite mandibular foramen are common (Bown, 1980, Minwer-Barakat et al., 2020). In *Mygalea*, there are two mental foramina: a large one below the posterior root p4/anterior root m1, and the front mental foramen is smaller and lies in the upper part of the horizontal ramus under the canine (Van den Hoek Ostende and Fejfar, 2006). The GFS dentary has one large mental foramen under the posterior alveolus of p4.

The morphology of the GFS materials is unique among fossil talpids. The size of these teeth is comparable to that of extant desmans, and similar in size to the largest fossil forms (Table 3). Though reminiscent of desmans, the upper molars (ETMNH 20747 and ETMNH 20779) do not possess all the synapomorphies that have been used to define the tribe; however, all of the lower molar synapomorphies are present in the holotype m2 (ETMNH 6994). Thus, these specimens are interpreted as representing a new occurrence of a stem desman, outside crown-group desmans.

Additionally, the holotype right m2 and right M1 can occlude. The second shear facet on the posterior aspect of the M1s line up with the second shear facet on the m2 (Figure 4). The holotype m2 also fits within the alveoli of the referred edentulous dentary (ETMNH 21077), supporting referral of that specimen. While these specimens fit together, they were recovered from different locations, suggesting they come from two different individuals.

Tribe SCALOPINI Trouessart, 1897
Genus *PARASCALOPS* True, 1894

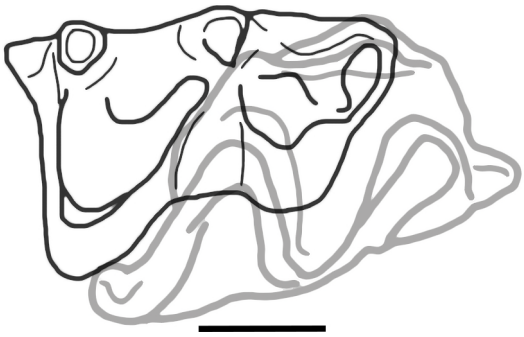

FIGURE 4. M1 (ETMNH 20779) super-positioned on top of m2 (ETMNH 6994). Scale bar equals 1 mm.

Parascalops grayensis sp. nov.
Figure 5A – F and Figure 6A - J

zoobank.org/942FCF9D-D9FD-4A70-9B12-D09C1DCE5476

Type material. ETMNH 6939 - left humerus.
Paratypes. ETMNH 6940 - right humerus; ETMNH 12305 - left humerus; ETMNH 20736 - right humerus; ETMNH 20782 - right humerus; ETMNH 14849 - left radius; ETMNH 20739 - right ulna; ETMNH 20754 - right ulna, missing distal end and olecranon process; ETMNH 20748 - nearly complete disarticulated left manus with six carpals (scaphoid, lunar, capitate, trapezium, triquetrum, and ulnar sesamoid?), three metacarpals (III, IV, and V), four proximal phalanges (I, III, IV, V), four medial phalanges (II-V), five terminal phalanges (I-V), and a partial right manus with three carpals (capitate, trapezium, and ulnar sesamoid?); ETMNH 24662 left M3.
Type locality. Gray Fossil Site, TN, USA.
Etymology. Species named for the locality where it was discovered.
Diagnosis. Entepicondylar foramen of the humerus is small and laterally positioned; pectoral tubercle is a large ridge, centrally positioned and extends almost half of entire diaphysis length; pectoral tubercle is robust; capitulum is smaller and angled 20-30 degrees superiorly; ulna and radius are large and robust.
Description. The humerus is longer than broad (Figure 5A - B; Table 4). The greater tuberosity is large and pronounced. There is a thin separation between the greater tuberosity and the humeral head. The brachialis fossa is triangular in shape. The teres tubercle is relatively large and curved proximally. There is a large gap between the entepicondylar process and the teres tubercle. The capitulum is parallel with the trochlea. The trochlea

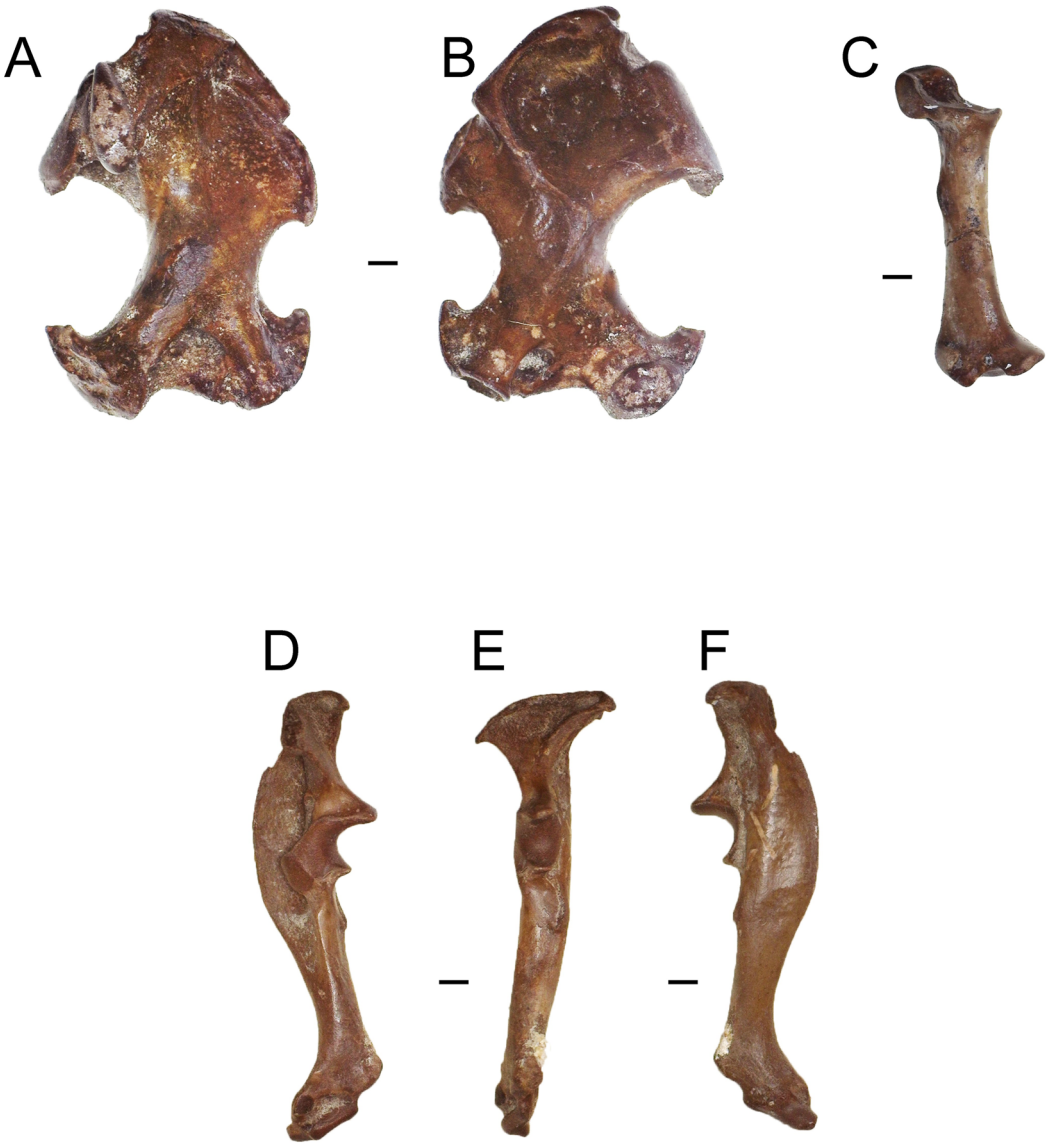

FIGURE 5. *Parascalops grayensis* sp. nov. material. ETMNH 6939, left humerus - A) posterior and B) anterior views. ETMNH 14849, right radius - C) medial view. ETMNH 20748, right ulna - D) medial, E) anterior, and F) lateral views.

touches the fossa of the *M. flexor digitorum* ligament. The pectoral tubercle is positioned proximally and can be either a large oval tubercle (ETMNH 6940, 12305, 14849) or a thin ridge (ETMNH 6939, 20736, and 20782). The scalopine ridge is weakly developed, and visible in several specimens (ETMNH 6939, 20736, and 20782).

In the radius (ETMNH 14849, Figure 5C), the capitular head is mediolaterally broad with a flat, square edge. The lunar articular facet is quite large, has a curved edge, and somewhat deep. The *M. abductor pollicis* tendon groove is at a sharp angle. The distal end is large and flares mediolaterally. There is a clean break through the center of the diaphysis that was repaired. There is no evidence of healing on this break suggesting it occurred post-burial. The distal end of the radius is relatively swollen.

The ulnae are short, mostly straight, and very robust (Figure 5D - F). The proximal olecranon crest forms a sharp angle with the shaft and a large blade greatly separated from the semilunar notch. The abductor fossa is enlarged. The semilunar notch is very well defined (appears as a strong semicircle). There is a large and curved medial olecranon crest. The triceps scar is large and rela-

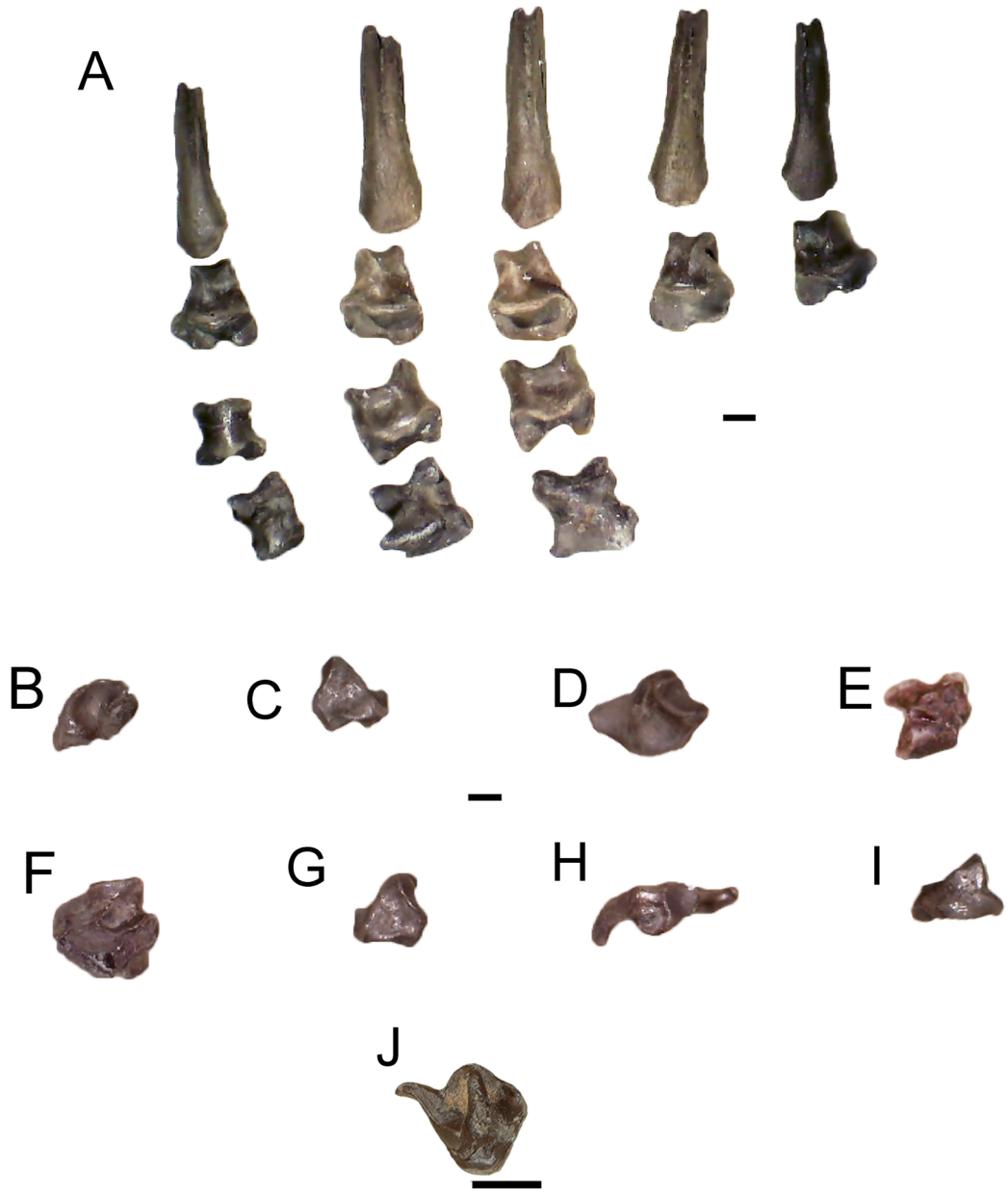

FIGURE 6. *Parascalops grayensis* sp. nov. material. ETMNH 20748, nearly complete disarticulated manus parts in dorsal view, A) articulated phalanges with claw cores (digits V - I), B) right trapezium, C) right capitate, D) right ulnar sesamoid, E) left scaphoid, F) left lunar, G) left triquetrum, H) left capitate, and I) left trapezium. ETMNH 24662, left M3 - J) occlusal view. Scale bars equal 1 mm.

tively wide. The abductor scar is elongate and makes up part of the base of the lateral olecranon crest. The distal end and the olecranon process are missing from ETMNH 20754.

There is one nearly complete manus (ETMNH 20748, Figure 6–A - I). All elements are completely disarticulated. There are eight carpals, five metacarpals, nine proximal and medial phalanges, and five terminal phalanges. All manus elements are large and robust. The carpals are blocky and large. The metacarpals and phalanges are short, anteroposteriorly compressed and mediolaterally broad. The terminal phalanges are elongate, broad, and bifurcated by large nutrient foramina.

TABLE 4. Postcranial Measurements for *Parascalops grayensis* sp. nov. Measurements in mm. * indicates incomplete specimens.

	Humerus					Radius			Ulna	
ETMNH specimen	Total length	Proximal width	Distal Width	Greater tuberosity	Lesser tuberosity	Total length	Width of lunar articular facet	Diaphysis length	Total length	Length without olecranon process
6939	14	8.81	8.67	5.92	4.66	-	-	-	-	-
6940*	14.9	10.59	8.4	6.46	5.35	-	-	-	-	-
12305*	10.57	-	-	-	-	-	-	-	-	-
20736*	14.76	10.41	8.31	6.68	5.75	-	-	-	-	-
14849	-	-	-	-	-	11.21	2.34	9.44	-	-
20754	-	-	-	-	-	-	-	-	18.09	14.19

There is one tooth referred to this taxon, a left M3 (ETMNH 24662, Figure 6J). The lingual portion of the M3 has a large and prominent parastyle, a prominent and well-worn paracone that is connected via a continuous mesostyle to the distinctly smaller metacone. The labial portion of the tooth is dominated by a large protocone, which as a consequence of wear is fused to relatively small protoconule and metaconule. The M3 length is 1.72 mm and width is 1.86 mm.

Discussion. Osteological characters that distinguish *Parascalops breweri* (Hairy-tailed mole) from all other known talpids include: the trochlea touches the fossa of the *M. flexor digitorum* ligament (Skoczeń, 1993), the brachialis fossa has a triangular shape (Hutchison, 1968), the fissure separating the greater tuberosity from the head is thin and subtle, the teres tubercle is about one-third the size of the pectoral ridge and has a strong curve, the scalopine ridge is weak and fragmentary with a prominence at about half of its length (Skoczeń, 1993), the position of the pectoral tubercle is proximal, the groove for the tendon of *M. abductor pollicis longus* on the radius is angled sharply, the top of the capitular process of the radius is square-shaped and flat, the medial olecranon crest of the ulna is more medial and has a strong medial curve, and the brachialis scar on the ulna is straight and thin. These characters are present on the GFS material, but morphology and size (Table 4) differences distinguish it from the extant species *Parascalops breweri*.

There are two described species within the genus *Parascalops*: *P. breweri* (extant) and *P. fossilis* from the Pliocene of Poland (Skoczeń, 1993). They are very similar in morphology but have some important differences. The characters differentiating *P. fossilis* from *P. breweri* are: 1) a significantly smaller humerus, 2) shallower fossa brachialis, 3) more oblique lesser tuberosity that passes the edge of the pectoral crest at a low angle that extends beyond the border of the humeral shaft, and 4) the medial vascular foramen on the diaphysis is larger (Skoczeń, 1993). The GFS material does not exhibit any of these morphological features.

The single tooth referred to *Parascalops grayensis* sp. nov., a left M3 (ETMNH 24662), is quite similar to studied specimens of *P. breweri*. The parastyle of the GFS specimen is larger than that of studied specimens of the extant *P. breweri*. Also, the angle between the parastyle, paracone, and mesostyle is more open in the GFS specimen than the extant species. Due to the lack of described dental material of *P. fossilis*, the GFS specimen could not be compared to that taxon.

Parascalops grayensis sp. nov. is similar in size (Table 5) and general morphology to *P. breweri*, but there are a few distinct differences. Evaluating the humerus of *Parascalops grayensis* sp. nov., the entepicondylar foramen is smaller and more laterally positioned on the diaphysis, the pectoral tubercle is a large, robust ridge, centrally positioned and almost half of entire diaphysis length,

TABLE 5. Comparing Sizes of all Species of *Parascalops*. Measurements in mm. * indicates incomplete specimens.

Taxon	Humerus length	Ulna length	Radius length
Parascalops breweri	12.3 - 15.4 (n = 22)	12.73 - 13.45 (n = 12)	8.67 - 10.11 (n = 11)
Parascalops fossilis	10.70 (n = 2)	--	--
Parascalops grayensis sp. nov.	13.48 - 15.52 (n = 4)	13.33* - 14.34 (n = 2)	10.26 (n = 1)

and the capitulum is smaller and angled 20-30 degrees superiorly from the ectepicondylar process. *Parascalops breweri* humeri typically have a large entepicondylar foramen that is more medially positioned, the pectoral tubercle is a prominent lump on the diaphysis, not a ridge, and the capitulum is relatively large and angled parallel to the ectepicondylar process. The ulnae and radii of *P. grayensis* sp. nov. are larger and more robust (Table 4). Muscle scars on these elements are more pronounced and have more rugose texture. The distal ends of these elements also appear more swollen than those of *P. breweri*.

Parascalops grayensis sp. nov. can be differentiated from *Parascalops fossilis* by size (Table 5) and general morphology. The humerus of *Parascalops grayensis* sp. nov. is large, the fossa brachialis is deep, the greater tuberosity is longer and more robust, the pectoral tubercle is large, robust and forms a ridge, and the entepicondylar foramen is small and laterally positioned. *Parascalops fossilis* has a shallow fossa brachialis, a smaller, less robust greater tuberosity, a small (almost non-existent) pectoral tubercle, and a relatively large, medially positioned entepicondylar foramen.

Parascalops grayensis sp. nov. is morphologically similar to, and falls within the biogeographic range of, extant *P. breweri*. This taxon may be ancestral to the extant species. These fossils represent the first pre-Pleistocene record of the genus in North America and earliest record globally. This extends the known fossil history for the genus by 4 million years in North America.

Genus *MIOSCALOPS* Ostrander et al., 1986
Mioscalops sp. Ostrander et al., 1986
Figure 7A - C

1960 *Scalpoides*; Wilson, p. 43, fig. 34-39, 42-46
1968 *Scalopoides*; Hutchinson, p. 58-80
1968 *Mioscalops*; Ostrander; Mebrate; Wilson, p. 9
2000 *Wilsonius*; Kretzoi and Kretzoi, p. 427

Type. *Mioscalops isodens*, left lower haw with i3-p1, p4-m2, No. 10067, University of Kansas Museum of Natural History, Pawnee Creek Formation, late Arikareean NALMA.

Referred specimens. ETMNH 6941 - left humerus; ETMNH 6942 - left humerus; ETMNH 6943 - left humerus, distal end; ETMNH 9565 - right humerus, distal end; ETMNH 10345 - left humerus, distal end; ETMNH 16024 - right humerus; ETMNH 20738 - right ulna; ETMNH 20740 - right humerus; ETMNH 20743 - left humerus, distal end; ETMNH 20744 - right humerus; ETMNH 20745 - right humerus, distal end; ETMNH 20971, right humerus.

Locality. Gray Fossil Site, TN, USA.

Description. The humeri of this genus have a long, gracile diaphysis with ends that do not flare as mediolaterally (Table 6) as in extremely fossorial moles. In the posterior view of the humerus (Figure 7A), the ectepicondylar and entepicondylar processes are angled sharply. The entepicondylar process is more robust than the ectepicondylar process. The ectepicondylar process projects laterally at a higher angle. The trochlea is mediolaterally elongated. The bicipital groove is angled medially. The teres tubercle is connected to the greater tuberosity via a thin ridge, which has a well-defined and relatively large bicipital groove. The humeral head is relatively large when compared to other talpid taxa. The radial notch is a little depressed. The olecranon fossa is small and has an oval/teardrop shape. The capitulum is saddle shaped (convex inferiorly, concave superiorly). The entepicondylar foramen is large and oval.

In the anterior view (Figure 7B), the humerus has a long shaft, with relatively narrow ends, a saddle shaped capitulum, and small entepicondylar foramen. The position of the entepicondylar foramen is much closer to the medial aspect of the distal end. The pectoral tubercle can vary in shape from a tubercle (ETMNH 6943, 9565, 10345, 20740, 20744, and 20745) to a small ridge (ETMNH 6941, 6942, 16024, 20743, and 20971). The greater tuberosity is massive and not separated from the lesser tuberosity. The pectoral crest starts at the greater tuberosity and stops 2/3 of the way down the diaphysis. The pectoral ridge con-

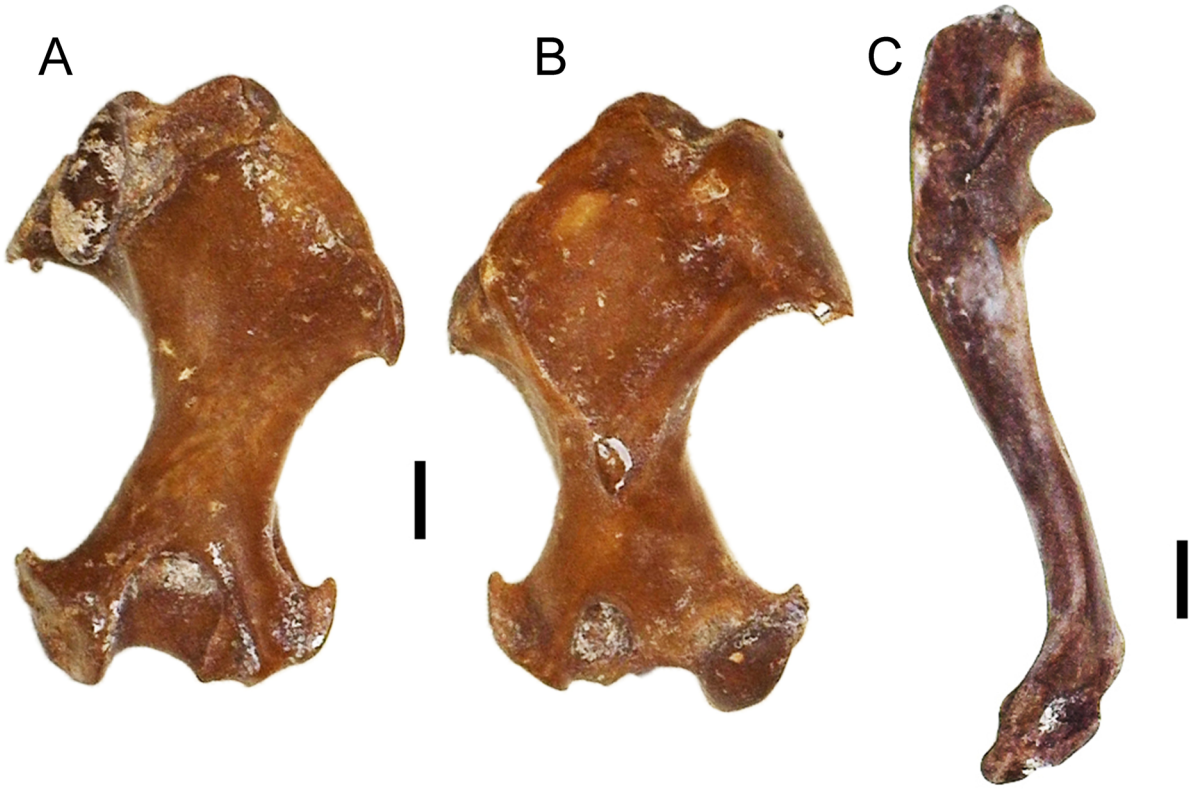

FIGURE 7. *Mioscalops* sp. skeletal material. ETMNH 6942, left humerus - A) posterior and B) anterior views. ETMNH 20738, right ulna - C) medial view. Scale bar equal 1 mm.

ceals most of the teres tubercle in the anterior view. There are small foraminae on either side of the pectoral ridge, near the base of the pectoral tubercle.

The ulna is almost complete, except that the olecranon process is broken off (Figure 7C). The distal end flares quite a bit. This ulna is very robust despite being so small. The diaphysis is long, relatively gracil, and mildly sinusoidal. There are no visible muscle scars along the diaphysis. Around the semilunar notch, the processus anconeus greatly overhangs the notch, but the coronoid process is quite pronounced as in more fossorial talpids. This trait is not common in semi-fossorial talpids.

Discussion. *Mioscalops* is the correct name to use when describing *Scalopoides* Wilson 1960. *Scalopoides* Wilson 1960, a common Miocene mole, is a

TABLE 6. Measurements for GFS *Mioscalops* sp. Measurements in mm. * indicates incomplete specimens.

	Humerus					Ulna	
ETMNH specimen	**Total length**	**Proximal width**	**Distal width**	**Greater tuberosity**	**Lesser tuberosity**	**Total length**	**Length without olecranon process**
20745*	4.48	-	3.60	-	-	-	-
6942	7.99	5.19	3.46	3.02	3.00	-	-
9565*	6.19	-	4.31	-	-	-	-
10345*	5.46	-	-	-	-	-	-
6941	8.16	5.23	4.06	3.38	3.24	-	-
20740	8.01	5.26	4.01	3.72	3.04	-	-
20738*	-	-	-	-	-	9.80	9.41

junior homonym of *Scalopoides* Bode 1953, a coleopteran from the Upper Lias of Europe. Therefore, the new name *Mioscalops* Ostrander et al. 1986 replaced *Scalopoides* Wilson 1960. Another genus, *Wilsonius* Kretzoi and Kretzoi 2000, was erected in Europe to describe the same Miocene talpid material; however, this genus is considered synonymous with *Mioscalops* Ostrander et al. 1986. Therefore, any talpid material being classified at the generic or species level as *Scalopoides* Wilson 1960 or *Wilsonius* Kretzoi and Kretzoi 2000, should be assigned to *Mioscalops* Ostrander et al., 1968.

Mioscalops has always been placed in the Scalopini tribe, but with little justification. Scalopini talpids are united by the presence of a scalopine ridge (Campbell, 1939); however, this "ridge" is actually a scar that runs parallel to the greater tuberosity on the diaphysis in the posterior view of the humerus (Hutchison, 1968). This character is also present in other tribes such as the Talpini, Urotrichini (Rzebik-Kowalska, 2014), and Scaptonychini (Skoczeń, 1980); therefore, it is not a reliable synapomorphy for the tribe Scalopini. Instead, researchers now rely on differences in dental characteristics to separate Scalopini talpids from other talpids (see Schwermann et al., 2019, S1 for a discussion of the dental formula). Recent geometric morphometric and phylogenetic analyses (e.g., Schwermann et al., 2019) have also placed *Mioscalops* within the Scalopini tribe, thus we do the same.

Mioscalops is most morphologically similar to *Scapanus*, *Condylura*, and *Scapanulus*. *Mioscalops* and *Scapanus* (Western North American moles) both have humeral heads that are in line with the diaphysis, the clavicular articular facet is semi-oval, a small teres tubercle, and a prominent scalopine ridge (Hutchison, 1968); however, the genus *Scapanus* includes three species of very robust scalopine talpids, and all documented fossil forms are similarly robust (Hutchison, 1968, 1974, 1987). GFS *Mioscalops* is not nearly robust enough to be considered *Scapanus*.

Mioscalops also shares similarities with *Condylura cristata* (star-nosed mole) in the proportions of the articular ends, the relative size of the teres tubercle, the shape of the humeral head, and the degree of overall robustness, but there are more differences between *Condylura* and *Mioscalops* than there are similarities. Some differences include: the direction of the humeral head, lack of scalopine ridge, clavicular articular facet being parallel to humerus long axis, strong separation from humeral head from clavicular facet, and a narrower trochlea in *Condylura* (Hutchison, 1968, 1984).

Mioscalops is morphologically similar to *Scapanulus oweni* (Gansu mole). They have similar humeral head orientations and sizes, a scalopine ridge, a broad trochlea, an absent channel separating the humeral head from the greater tuberosity, and the proximal end of the #Ilustrat tunnel is anteriorly visible (Hutchison, 1968). Differences in teres tubercle shape and size, as well as the size of the pectoral crest, differentiate *Mioscalops* from *Scapanulus*.

The name *Mioscalops* has commonly used as a "garbage-bin" taxon for any talpid found during the Miocene, but it is morphologically distinct from other Neogene talpid taxa. *Mioscalops* is known from the Oligo-Miocene through the Pliocene of North America and the Miocene of Europe (Gunnell et al., 2008). *Mioscalops* was widely distributed across North America making it the most common talpid to find in a Cenozoic fossil locality that contains talpids (Gunnell et al., 2008).

Tribe NEUROTRICHINI Hutterer, 2005
Genus *NEUROTRICHUS* Günther, 1880
Neurotrichus sp. Günther, 1880
Figure 8A - D

1858 *Urotrichus* Baird; Baird, p. 76

1880 *Neurotrichus* Günther; Günther, p. 440.

Referred specimens. ETMNH 4915 - left humerus, missing proximal end; ETMNH 10277 - left humerus, missing proximal end; ETMNH 9713 - left edentulous dentary; ETMNH 9728 - left posterior dentary fragment with m3; ETMNH 16023 - right m3; ETMNH 20737 - right dentary with m1-3; ETMNH 20741 - left dentary with m1-2; ETMNH 20862 - left dentary with m2; ETMNH 26996 - left dentary with m2; ETMNH 30380 - right dentary with m1.

Locality. Gray Fossil Site, TN.

Description. The dentary is thin and gracile with minimal curving along the inferior margin (Figure 8A - B; Table 7). The greatest point of curvature is below the talonid basin of m2 and the trigonid of m3. The anterior mental foramen is positioned under the p3 anterior alveolus (ETMNH 9713 and ETMNH 20741). There is a small gap between m3 and the ascending ramus. The angle between the ascending ramus and the horizontal ramus is approximately 90°.

The m1 trigonid is robust and elongate, with an anteriorly directed paraconid. The protoconid is the tallest cusp, and then metaconid, with the paraconid as the shortest cusp. The metaconid and

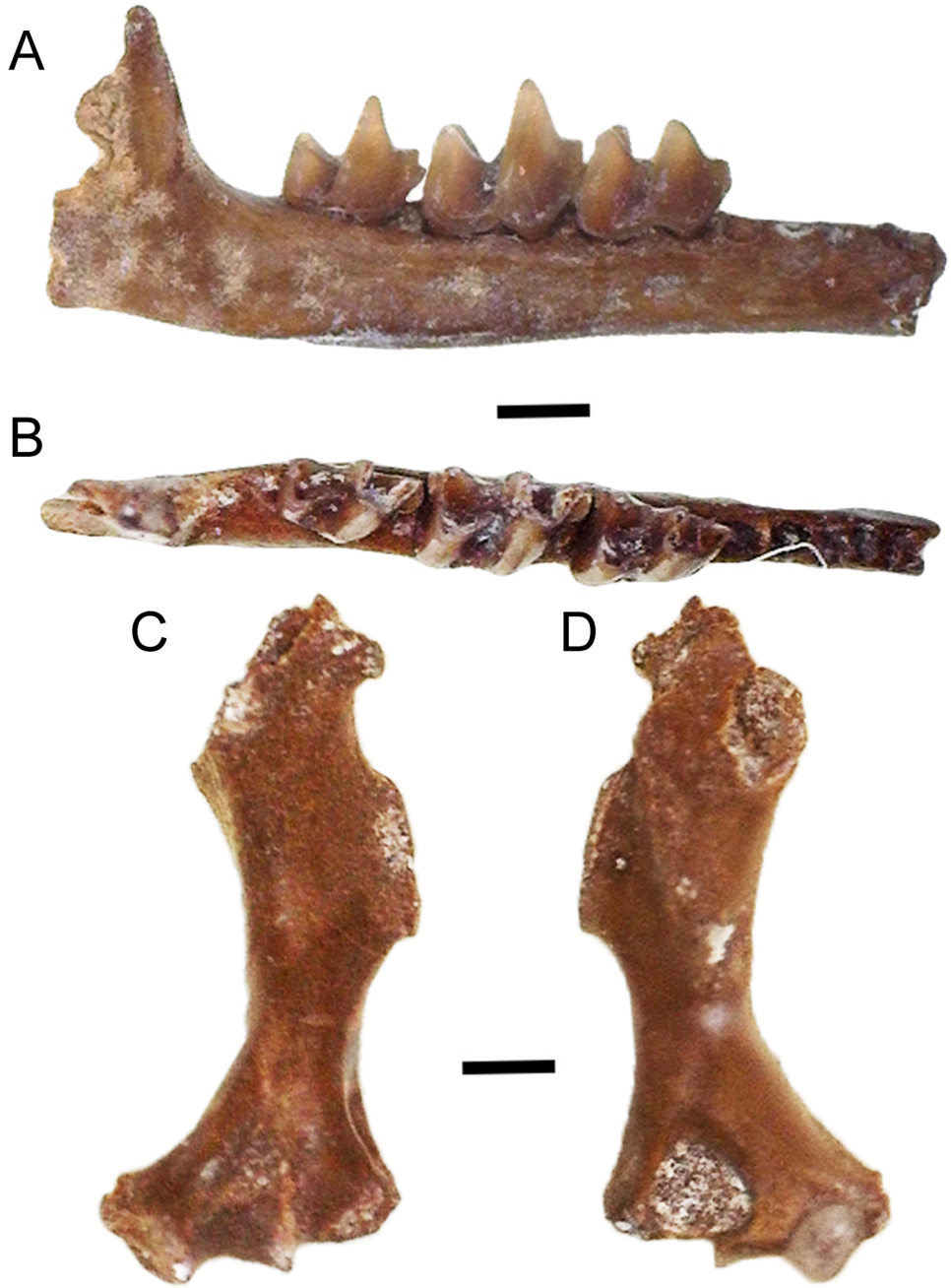

FIGURE 8. *Neurotrichus* sp. skeletal material ETMNH 20737, right dentary with m1-3 - A) lingual and B) occlusal views. ETMNH 4915, left humerus - C) posterior and D) anterior views. Scale bars equal 1 mm.

paraconid have wear on their buccal aspect. The paraconid has a bladed notch along its posterior aspect. In the m1, the talonid is buccolingually broad, and about the same size and height as the trigonid. The cristid obliqua terminates anteriorly (buccally) and is semi-separated by a small notch from the posterior wall of the trigonid. The entoconid and hypoconid are distinct. There is a small posterior accessory cusp (entostylid) on the posterior aspect of the entoconid. There is a strong hypoflexid between the hypoconid and protoconid. There is a well-formed entocristid between the entoconid and the metaconid. The postfossid is relatively deep, but not as deep as in the m2. The cingulids are not particularly prominent in the m1, with the precingulid, ectocingulid, and postcingulid

TABLE 7. Measurements for *Neurotrichus* sp. Tri is trigonid length. Tal is talonid length. All measurements in mm.

ETMNH specimen	Humerus		Teeth								
	Total length	Distal Width	m1			m2			m3		
			Width	Tri	Tal	Width	Tri	Tal	Width	Tri	Tal
20741	7.19	3.05	-	-	-	-	-	-	-	-	-
9728	-	-	1.57	0.91	1.04	1.69	0.98	1.08	-	-	-
9713	-	-	-	-	-	-	-	-	1.40	0.95	0.90
20737	-	-	1.6	0.94	1.14	-	-	-	1.46	0.94	0.90

present. and entocingulid absent. There is no mesoconid on any of the lower molars.

In the m2, the trigonid is taller than the talonid and anteroposteriorly smaller (Figure 8B). The protoconid is the tallest cusp of the trigonid, then metaconid, and the paraconid is the shortest cusp. The paraconid has a bladed notch along the posterior aspect. The talonid has a strong hypoconid and entoconid. The cristid obliqua is separated from the trigonid by a small notch. There is a tiny posterior accessory cuspid (entostylid) just posterior to the entoconid. There is a strong hypoflexid between the hypoconid and protoconid. The postfossid is very deep. An entocristid is present, but weak. Cingulids are similar to those of the m1, with precingulid, ectocingulid, and postcingulid present, but there is also a weak entocingulid

The m3 is broader anterioposteriorly than buccolingually (Figure 8B). The trigonid flares anterioposteriorly (paraconid and metaconid diverge from one another) making it appear very open. The paraconid has a bladed notch along the posterior aspect. The talonid is narrow and very open, and lower and smaller than the trigonid. There is a distinct hypoconid, and evidence for an entocristi in some specimens (not present in ETMNH 20737 but present in ETMNH 16023 and ETMNH 9728). The entoconid is large and has a well-formed posterior accessory cuspid (entostylid) present. There is no hypoconulid.

The humerus is quite gracile (Figure 8C - D); it is long and thin with minimal flaring projections on the distal end (Table 7). The pectoral ridge narrows to a point about halfway down the diaphysis. ETMNH 10277 has a less prominent pectoral ridge present on the diaphysis than ETMNH 4915. The teres tubercle is long, relatively robust, and rather rectangular. In the anterior view, the olecranon fossa has a distinct concave notch at the base towards the center. The olecranon fossa is horseshoe shaped and asymmetrically slanted medially. In the posterior view, the trochlea is relatively dorsoventrally elongate and mediolaterally narrow. There is a groove in between the trochlea and the entepicondylar process along the distal-most aspect of the humerus. This gives the distal end of the humerus an asymmetrical appearance. The medial epicondyle is rather robust and probably had a large process on it. The entepicondylar foramen is visible just above the medial epicondyle and is quite large. The ectepicondylar foramen is very large. The entepicondylar process is a small projection sticking off the medial aspect. The capitulum is very small and oval-shaped.

Discussion. The teeth of shrew moles tend to be brachydont, and the upper molars have a small accessory cuspule (Skoczeń, 1980) that resembles and functions like a hypocone. The lower molars usually have a posterior accessory cuspule, like Desmanini talpids. The size of the accessory cuspule varies depending on the tooth and taxon, but it is quite large in the tribe Urotrichini. All shrew moles have a distinct bladed crest along the posterior aspect of the paraconid in all three lower molars.

Recent morphological analysis by Rzebik-Kowalska (2014) and Sansalone et al. (2016) have yielded recognition of three genera within Neurotrichini, the extant *Neurotrichus* and fossil *Quyania* and *Rzebikia*. The teeth, dentary, and humeri of these taxa show some clear similarities, but have a number of diagnostic differences (Rzebik-Kowalska, 2016; Sansalone et al., 2016). The known teeth and humeri of *Rzebikia* are similar in size to extant *Neurotrichus*, but larger than *Quyania*.

The genus *Quyania* is defined by having a gracile trigonid, mesoconid on m1, crista obliqua of the m1 terminate anteriorly (buccally) and separated by a small notch from the posterior wall of the trigonid, and anterior mental foramen lying under the p2 (Storch and Qui, 1983; Rzebik-Kowalska, 2014). The genus *Rzebikia* has a number of features intermediate between the other genera, and is defined, in part, by having reduced cingula on all three lower molars, variably present mesoconids, variable separation of the cristid obliqua from the trigonid via a small notch, variable anterior mental foramen position, and entoconids of both m1 and

m2 robust and displaced lingually making the lingual side of the molars concave (Sansalone et al., 2016). In *Neurotrichus*, the m1 trigonid is more robust and anteroposteriorly elongate, the mesoconid is absent, the cristid obliqua is slightly separated from the trigonid without a notch, lower molar cingula are present, and the anterior mental foramen is under the anterior root of the p3. The upper and lower teeth of *Rzebikia* and *Quyania* are wider and lower-crowned than the teeth of *Neurotrichus*. The orientation of the ascending ramus of the dentary relative to the horizontal ramus also shows differences, with a 90° angle in both *Neurotrichus* and *Rzebikia*, and >90° angle in *Quyania*.

The humeral morphology of *Rzebikia polonica* resembles that of *Quyania chowi*, *Neurotrichus gibbsii* (American shrew mole), *Urotrichus talpoides* (Japanese shrew mole), and *Dymecodon pilirostris* (True's shrew mole). All of these taxa have similar general morphology: a long, gracile humeral diaphysis with enlarged teres tubercle, reduced greater tuberosity, reduced lesser tuberosity that also projects medially, and deep bicipital groove (Sansalone et al., 2016); however, all species in *Quyania* have a small notch between the pectoral ridge and the teres tubercle (Storch and Qui, 1983), while the extant species do not have this feature. The humerus of *R. polonica* can be differentiated from that of *Q. chowi* based on a more robust shaft and a more prominent "scalopine ridge" (Rzebik-Kowalska, 2014; Sansalone et al., 2016).

Comparisons of these taxa by several authors (Storch and Qiu, 1983; Rzebik-Kowalska, 2014; Sansalone et al., 2016) suggest *Rzebikia polonica* fits in an ancestor - descendant relationship with *Q. chowi* and could belong to one phyletic lineage of Old World moles, though its affiliation with *Neurotrichus* or *Quyania europaea* is still uncertain (Skoczeń, 1980, 1993; Sansalone et al., 2016).

The GFS shrew mole described here has characteristics that clearly indicate it is a member of the Neurotrichini, and has features that allow referral to the genus *Neurotrichus*. Like both *Quyania* and *Neurotrichus*, cingula are present on all lower molars, though they are not strongly developed. The m1 trigonid is elongate with a relatively anteriorly directed paraconid, which is characteristic of *Neurotrichus*. The lower molars lack mesoconids, like *Neurotrichus* and some specimens of *Rzebikia*. The cristid obliqua of the m1 is semi-separate from the trigonid, with only a small notch, similar to some specimens of *Rzebikia* and *Neurotrichus*. Entoconids of the lower molars are relatively large, but they are not lingually displaced to yield a concave lingual surface of the tooth, as is typical of *Rzebikia*. The anterior mental foramen lies below the anterior root of the p3, as in *Neurotrichus* and some specimens of *Rzebikia*. The orientation of the ascending ramus in the GFS shrew mole (90° angle to horizontal ramus) is similar to that of both *Neurotrichus* and *Rzebikia*.

Based on this combination of characters, the GFS shrew mole is referred to *Neurotrichus*, though the fragmentary nature of the remains precludes more refined taxonomic assignment. The absence of a complete proximal humerus in the GFS shrew mole sample precludes direct comparison to some characteristics considered diagnostic of the other neurotrichine taxa (Sansalone et al., 2016).

GEOMETRIC MORPHOMETRIC RESULTS

Relative Warps Analysis

Relative warp analysis yielded 3 relative warp axes that account for 88.26% of variance in humerus shape (Figure 9). Relative warp 1 (RW1) accounts for 78.75% of total variation in humerus shape. Positive scores for RW1 are associated with a reduced greater tuberosity, an elongated lesser tuberosity, a proximodistally reduced, mediolaterally elongate teres tubercle, and greater mediolateral elongation of the distal end, greatly mediolaterally compressed diaphysis, and enlarged lesser and greater sulci. Negative scores for RW1 are associated with an enlarged greater tuberosity, a reduced lesser tuberosity, a proximodistally elongate mediolaterally reduced teres tubercle, and mediolateral compression of the distal end, reduced and laterally oriented head of capitulum, and reduced trochlea.

Relative warp 2 (RW2) accounts for 6.28% of total variance. Positive scores for RW2 are associated with reduction of the greater and lesser tuberosities, an elongation of the teres tubercle, an enlarged trochlea and capitulum, mediolaterally compressed proximal and distal ends, the entire humerus is oriented more laterally with the deltoid process in line with the medial-most aspect of the capitulum. Negative RW2 scores are associated with elongation of both the greater and lesser tuberosities, a reduction in the teres tubercle, and greatly reduced trochlea and capitulum, mediolaterally elongate proximal and distal ends, and proximodistally compressed diaphysis.

Relative warp 3 (RW3) accounts for 3.23% of total variance. Positive score for RW3 are associ-

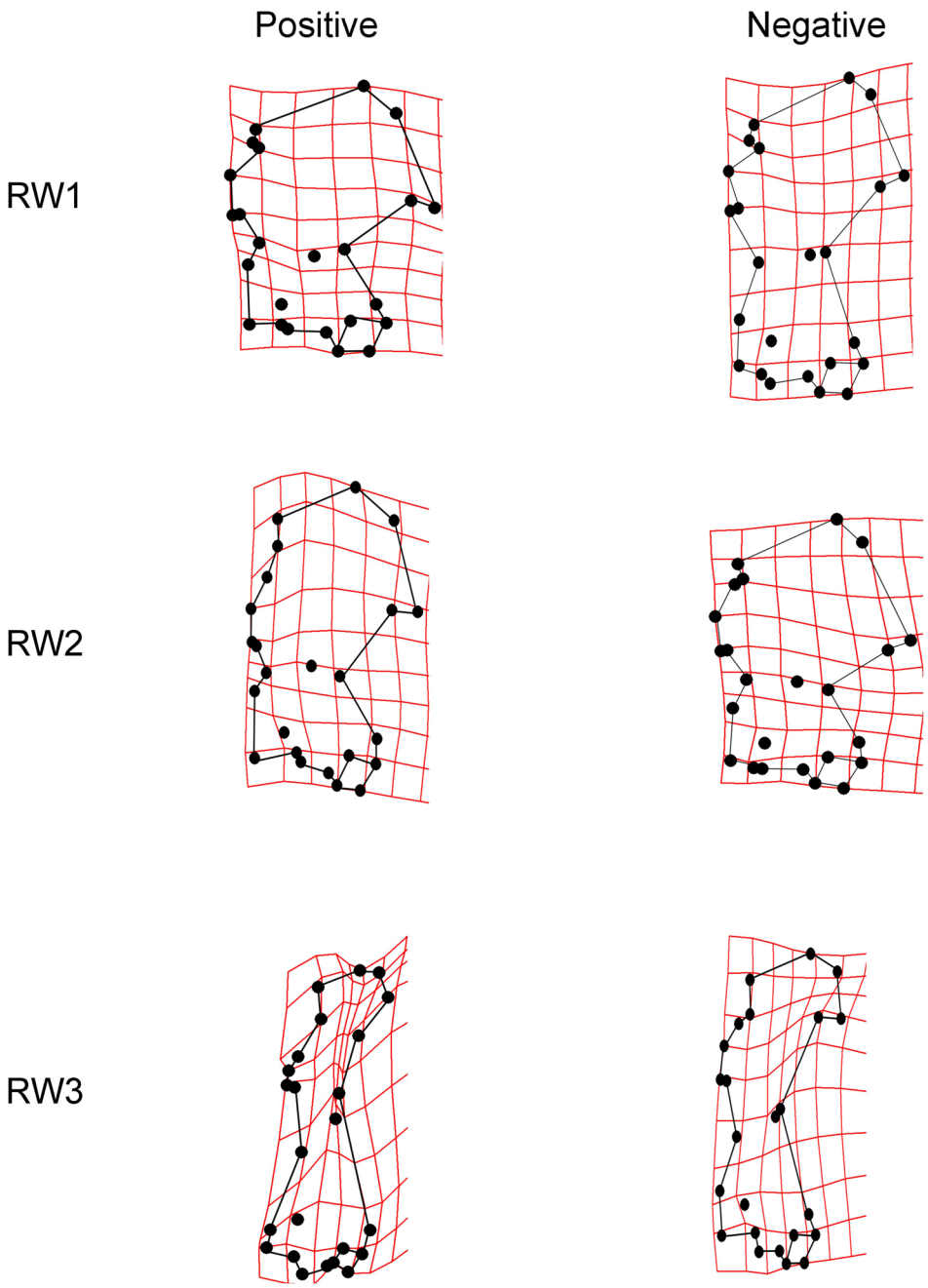

FIGURE 9. Relative warps analysis thin plate splines showing grid deformation in positive and negative directions to achieve change in humerus shape per relative warp. The consensus shape per relative warp is shown in the center.

ated with proximodistally reduced teres tubercle, reduced trochlea, enlarged and laterally oriented capitulum, well-developed deltoid process, and medial-most edge of the greater tuberosity that does not overhang the medial-most edge of the capitulum. Negative RW3 scores are associated with a slightly reduced lesser tuberosity, greatly mediolaterally elongated teres tubercle, more laterally positioned trochlea, reduced and medially oriented capitulum, very reduced deltoid process, and mediolaterally compressed diaphysis.

Canonical Variate Analysis

The canonical variate analysis using partial warp scores as variables yielded three canonical variates, which explained 100% of the variance in humerus shape and found significant separation of locomotor groups (Wilks' $\lambda = 0.001$, $P < 0.001$)

TABLE 8. Eigenvalues, % Variance of Axes, and Wilks' Lambda for CVA.

Function	Eigenvalue	% of Variance	Canonical Correlation	Wilks' Lambda	Significance
CV1	35.635	75.0	0.986	0.001	0.000
CV2	10.244	21.6	0.954	0.034	0.000
CV3	1.362	3.4	0.787	0.380	0.000

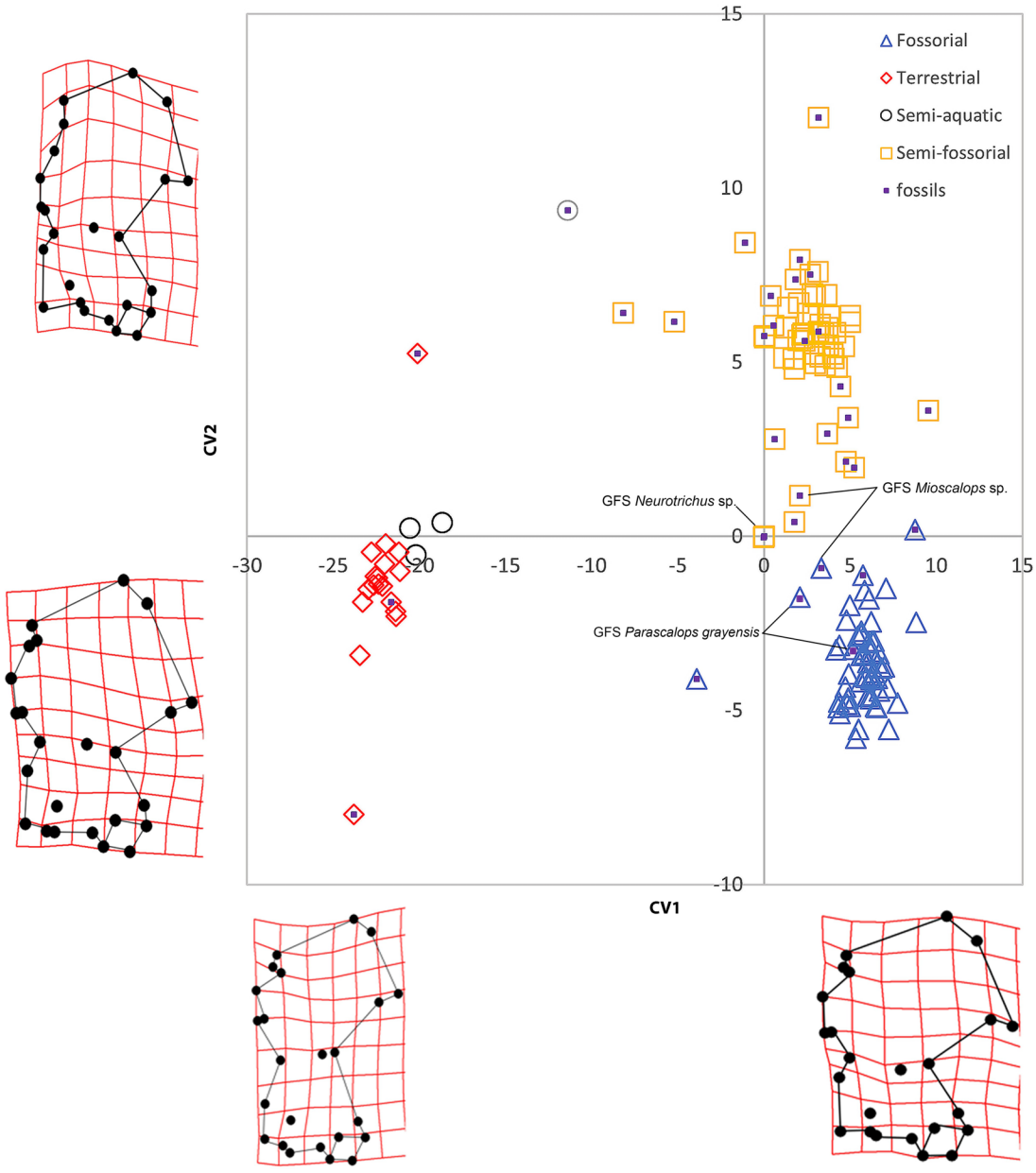

FIGURE 10. Plot of humerus shape based on canonical variates one (CV1) and two (CV2). Deformation grids show change in shape along each axis in positive and negative directions. Fossils taxa have a purple square in the center. GFS taxa are labeled.

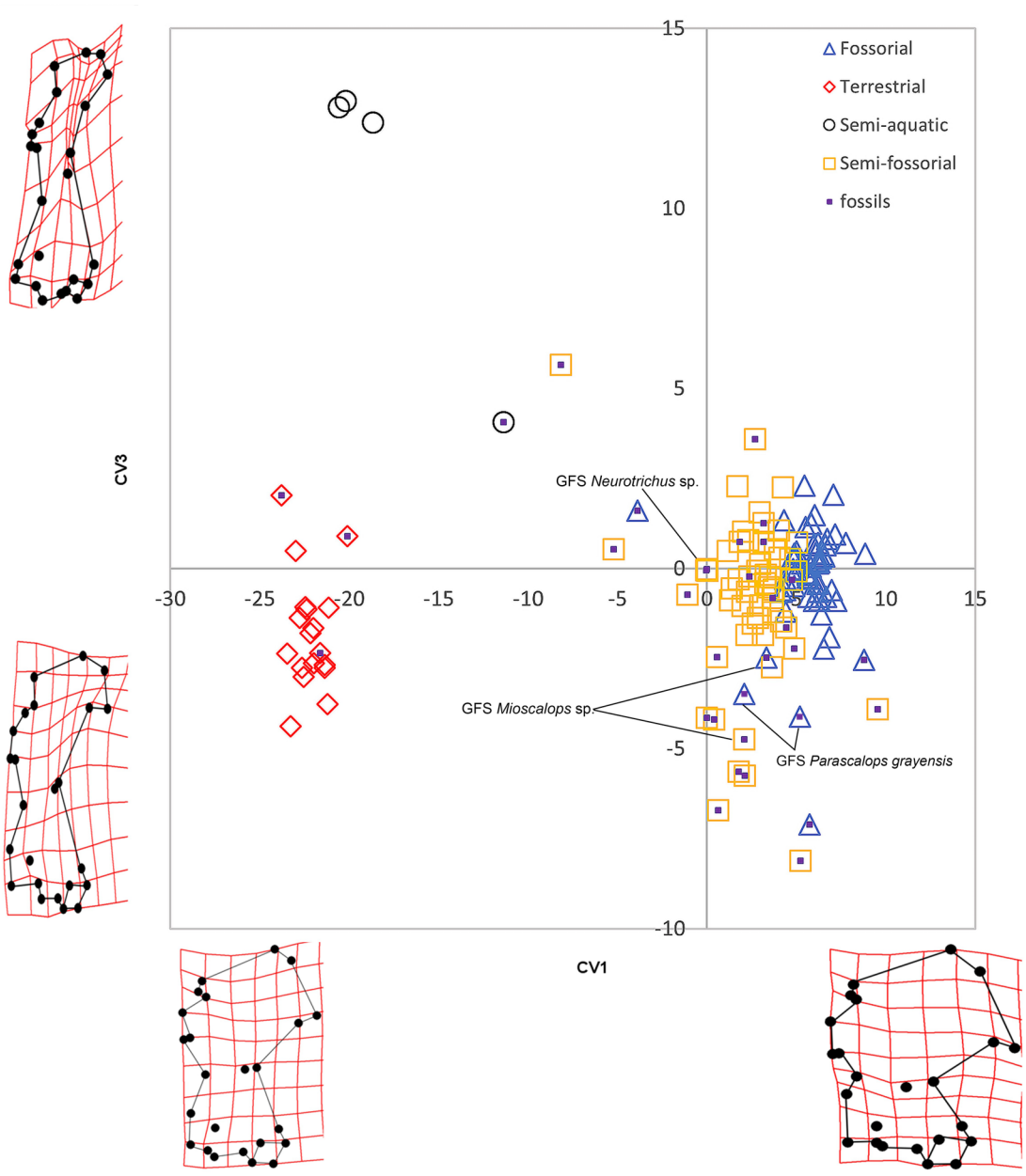

FIGURE 11. Plot of humerus shape based on canonical variates one (CV1) and three (CV3). Deformation grids show change in shape along each axis in positive and negative directions. Fossils taxa have a purple square in the center. GFS taxa are labeled.

(Table 8); Canonical Variate 1 (CV1) accounts for 75% of the variance and separates fossorial taxa from non-fossorial ones (Figures 10 and 11). CV1 separates fossorial talpids, with humeral diaphysis compression and articular end elongation, at the positive end from non-fossorial talpids, with humeral diaphysis elongation and articular end compression, at the negative end. The teres tubercle is proximodistally compressed, the deltoid process is sharp and angled distally, the pectoral tubercle is more medially positioned and more distally placed on the diaphysis, the fossa for the *M. flexor digitorum* ligament is more distal at the positive end compared to teres tubercle elongation, weakly angled deltoid process, more centrally and laterally placed pectoral tubercle, and the entepicondylar foramen is more proximal at the negative end.

Canonical Variate 2 (CV2) has the second highest variance at 21.6% and separates fossorial taxa from semi-fossorial taxa (Figure 10). CV2 separates semi-fossorial forms, with more mediolateral

TABLE 9. Canonical Variates Analysis Classification for All Talpids.

			Predicted Group Membership				
		Category	Fossorial	Terrestrial	Semi-aquatic	Semi-fossorial	Total
Original	Count	Fossorial	57	0	0	0	57
		Terrestrial	0	18	0	0	18
		Semi-aquatic	0	0	4	0	4
		Semi-fossorial	1	0	0	55	56
	%	Fossorial	100.0	0.0	0.0	0.0	100.0
		Terrestrial	0.0	100.0	0.0	0.0	100.0
		Semi-aquatic	0.0	0.0	100.0	0.0	100.0
		Semi-fossorial	1.9	0.0	0.0	98.1	100.0
Cross-validated	Count	Fossorial	57	0	0	0	57
		Terrestrial	0	16	2	0	18
		Semi-aquatic	0	0	3	1	4
		Semi-fossorial	2	0	1	53	56
	%	Fossorial	100.0	0.0	0.0	0.0	100.0
		Terrestrial	0.0	88.9	11.1	0.0	100.0
		Semi-aquatic	0.0	0.0	75.0	25.0	100.0
		Semi-fossorial	3.7	0.0	1.9	94.4	100.0

compression of the proximal end, a larger bicipital groove, more distally positioned teres tubercle, and mediolateral elongation of the distal end, at the positive end from fossorial specialists, with mediolaterally flaring proximal end, elongated greater tuberosity, reduced bicipital groove, proximally positioned teres tubercle, and mediolateral compression of the distal end, at the negative end. On the positive end, the entepicondylar foramen is positioned more laterally relative to the trochlea, whereas the entepicondylar foramen is in line with the lateral margin of the trochlea at the negative end.

Canonical Variate 3 (CV3) accounts for only 3.4% of variance and separates terrestrial taxa from semi-aquatic taxa (Figure 11). CV3 separates semi-aquatic forms, with proximodistal elongation of the diaphysis, major reduction of the proximal and distal ends, reduced teres tubercle, and reduced capitulum, at the positive end from more terrestrial forms, with less proximodistal elongation, mediolateral flaring of proximal and distal ends, and well-developed teres tubercle and capitulum, at the negative end.

The analysis correctly classified locomotor groups in 99.2% of original grouped cases and 95.5% when cross-validated (Table 9). Over half (n=17) of the fossil taxa were classified as semi-fossorial (Table 10), but a few classified as semi-aquatic (n = 1) and terrestrial (n = 2). GFS *Neurotrichus* sp. specimens were classified as semi-fossorial. GFS *Mioscalops* sp. specimens were classified as both semi-fossorial and fossorial, while GFS *Parascalops grayensis* sp. nov. specimens were classified as fossorial.

Classifications of fossil taxa resulted in high posterior probabilities and low conditional probabilities (Table 10). This indicates that fossil taxa are close to the centroid for a particular group (high posterior probability), but outside of the observed clustering for that group (low conditional probability), as indicated by their intermediate positions in morphospace.

Hierarchical Cluster Analysis

Using Hierarchical Cluster Analysis, two phenograms were generated: one depicting all individuals included in the analysis and the other based on species mean values for partial warps. In the individual phenogram (Figure 12), almost all of the species within the same genus clustered together, though there were not enough variables to prevent large polytomies. There are a few genera with species that clustered into different groups, such as *Urotrichus soricipes* grouping with Soricidae and the Desmanini rather than the other shrew moles [Scaptonychini, Urotrichini, and Neurotrichini], and

TABLE 10. Classification of Fossils. P(D/G) represents the conditional probability of the observed discriminant function score, given membership in the most likely group. P(G/D) represents the posterior probability that a case belongs to the predicted group, given the sample used to create the discriminant model.

Case	Taxon	Predicted group	P(D>d | G=g)	P(G=g | D=d)
88	*Condylura kowalskii*	Semi-fossorial	0.291	1.000
89	*Desmanella gudrunae*	Terrestrial	0.749	1.000
90	*Desmanodon crocheti*	Semi-fossorial	0.244	1.000
91	*Desmanodon fluegeli*	Semi-fossorial	0.921	1.000
92	*Gaillardia thompsoni*	Terrestrial	0.272	1.000
96	*Geotrypus montisasini*	Semi-fossorial	0.503	1.000
97	*Leptoscaptor robustor*	Fossorial	0.440	1.000
98	*Mioscalops* sp. ETMNH 6941	Semi-fossorial	0.211	1.000
99	*Mioscalops* sp. ETMNH 6942	Fossorial	0.122	1.000
100	*Mygalea magna*	Semi-aquatic	0.001	0.521
101	*Myxomygale minor*	Semi-fossorial	0.000	1.000
102	?*Rzebikia polonicus*	Semi-fossorial	0.351	1.000
103	*Parascalops grayensis* ETMNH 6939	Fossorial	0.009	1.000
104	*Parascalops grayensis* ETMNH 6940	Fossorial	0.561	1.000
105	*Parascalops fossilis*	Fossorial	0.253	1.000
106	*Proscapanus sansansiensis*	Semi-fossorial	0.327	1.000
107	*Quyania chowi*	Semi-fossorial	0.177	1.000
108	*Quyania* cf. *Q. europaea*	Semi-fossorial	0.088	1.000
109	*Quyania polonicus*	Semi-fossorial	0.645	1.000
110	*Mioscalops* sp. A	Semi-fossorial	0.120	1.000
111	*Mioscalops ripafodiator*	Semi-fossorial	0.228	1.000
112	*Mioscalops* sp. E	Semi-fossorial	0.270	1.000
113	*Tenuibrachiatum storchi*	Semi-fossorial	0.635	1.000
122	*Yanshuella primaeva*	Semi-fossorial	0.003	0.977
123	*Yunoscaptor scalprum*	Semi-fossorial	0.087	1.000
134	*Neurotrichus* sp. ETMNH 4915	Semi-fossorial	0.092	1.000
135	*Neurotrichus* sp. ETMNH 10277	Semi-fossorial	0.080	1.000

Quyania europaea clustering with *Dymecodon pilirostris* rather than the two species of *Quyania*.

The species mean phenogram (Figure 13) shows the average clustered position for each taxon. This phenogram has been color-coded to make comparisons with the He et al. (2016) phylogeny easier. There are six distinct clusters that resemble well-known tribes defined by He et al. (2016), but their positions differ slightly. The cluster analysis suggests Condylurini and the shrew mole cluster (Scaptonychini, Neurotrichini, and Urotrichini) are similar and that *Uropsilus* is morphologically separated from Talpinae, which agrees with the He et al. (2016) molecular hypothesis. The cluster analysis grouped *Uropsilus* (Uropsilinae), *Galemys* (Desmanini), and *Gaillardia* with Soricidae (true shrews represented by *Sorex* and *Blarina*) and grouped the Talpini and Scalopini clusters together.

The Gray Fossil Site taxa clustered with three separate groups: Scalopini (*Parascalops grayensis* sp. nov.), Urotrichini (*Neurotrichus* sp.), and Condylurini (*Mioscalops* sp.). GFS *Parascalops grayensis* sp. nov. clustered with all individuals in the genus *Parascalops*, which includes extant *P. breweri* and *P. fossilis*, along with *Proscapanus sansansiensis*. GFS *Neurotrichus* sp. clustered with *Quyania europaea* and extant *Dymecodon pilirostris*. GFS *Mioscalops* clustered with *Mioscalops* sp. E, *Yunoscaptor scalprum*, *Yanshuella primaeva*, *Scapanulus oweni*, *Mioscalops ripafodiator*, *Condylura kowalskii*, and *Condylura cristata*.

Both phenograms created by the cluster analysis verified that there are at least four distinct clus-

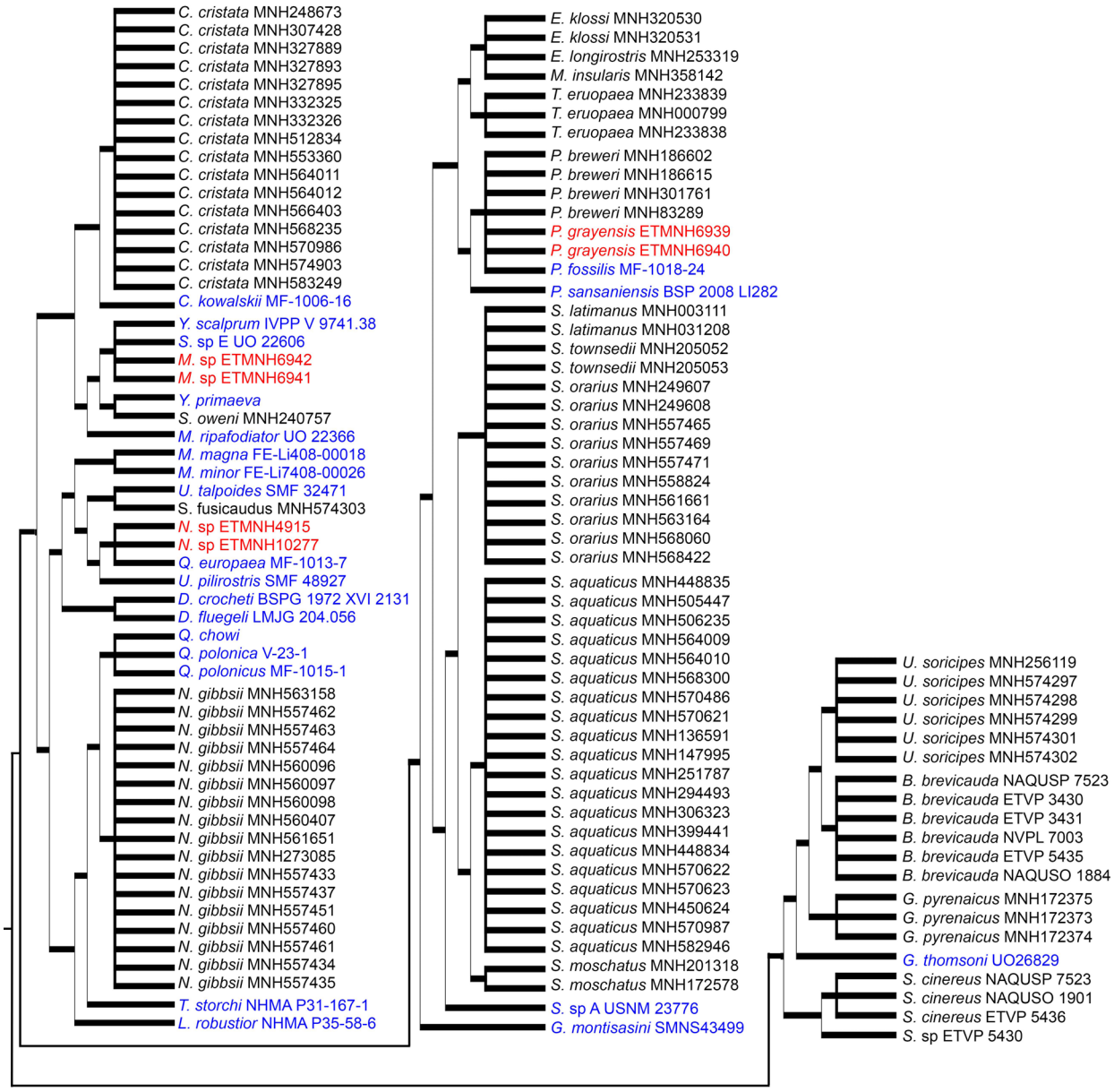

FIGURE 12. Individual taxon phenogram based on squared Euclidean distance. Fossil taxa are in blue. Gray Fossil Site taxa are in red.

ters, six if the two groups that clustered with the outgroup are included. The analysis clustered the Talpini and Scalopini groups together, but also shows distinct separation between the two from one another. The analysis was also able to recreate the shrew mole (Scaptonychini, Urotrichini, and Neurotrichini) and the Condylurini clusters.

DISCUSSION

Gray Fossil Site Ecology

At the Gray Fossil Site, there are at least four distinctly different talpids, each occupying a different ecological niche space. Not only is taxonomic diversity high, but also ecological diversity is higher than any other Pliocene-aged site in North America. There are two Miocene sites (Ash Hollow and McKay Reservoir), but no Pliocene sites, in North America that have comparable talpid diversity (FAUNMAP and MIOMAP, Carrasco et al., 2007;

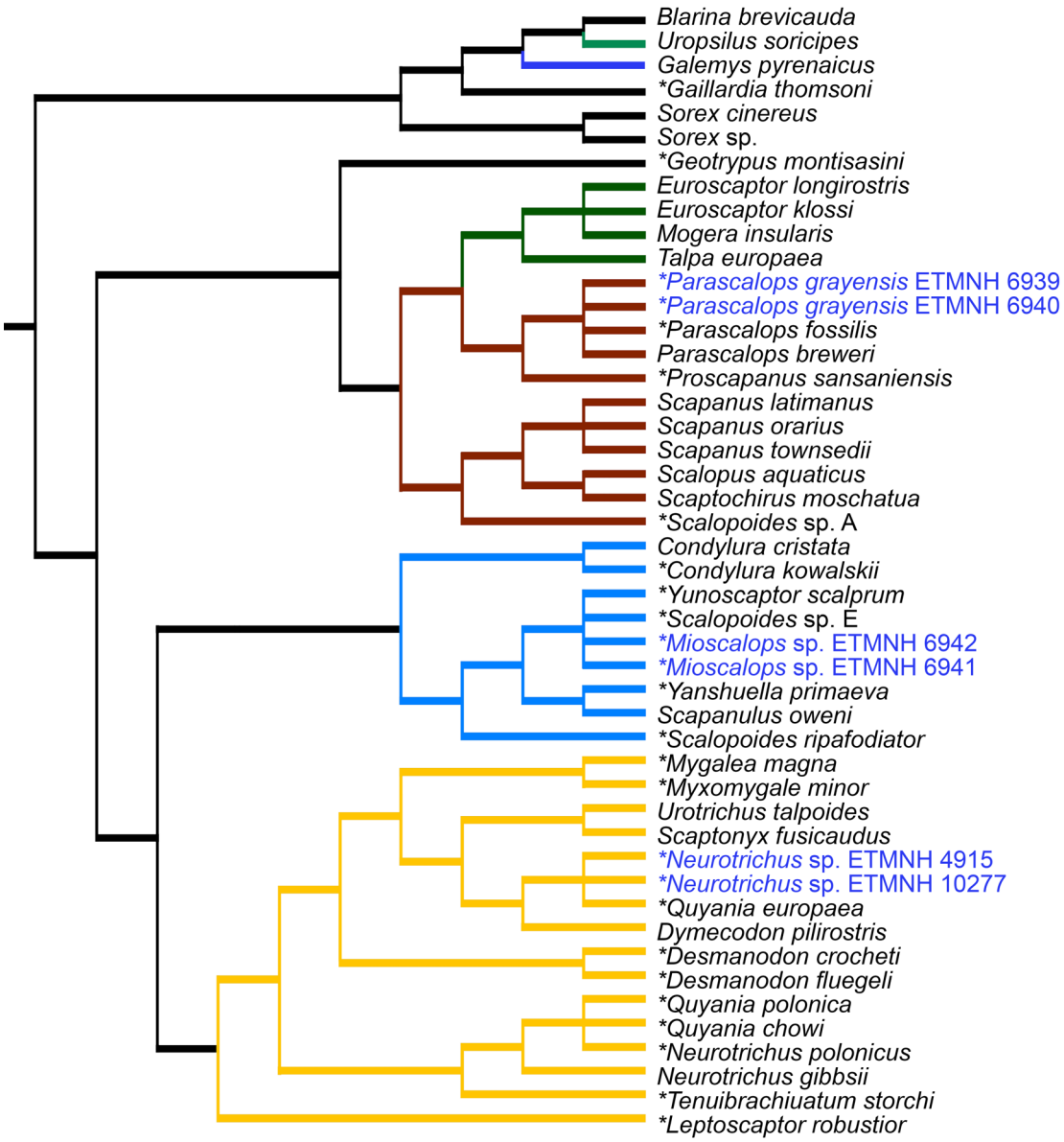

FIGURE 13. Average position phenogram. Major clusters color-coded to match He et al. (2016). GFS taxa in blue. * indicates fossil taxa.

Graham and Lundelius, 2010; http://www.ucmp.berkeley.edu/neomap/).

Desmanini. Extant desmans are semi-aquatic moles that spend most of their life hunting and foraging underwater. They have long, laterally compressed tails fringed with stiff hairs to retain body heat (Nowak and Paradiso, 1983; Palmeirim and Hoffmann, 1983; Gorman and Stone, 1990). When swimming, they propel themselves with their hindlimbs, and thus, have particularly heavily muscled hindlimbs and large, webbed hindfeet, when compared to other talpids (Palmeirim and Hoffmann, 1983; Gorman and Stone, 1990).

The desmans are specialized aquatic insectivores only living in Eurasia today. The Russian desman, *Desmana moschata*, prefers slow moving streams, lakes, and ponds while the Pyrenean desman, *Galemys pyrenaicus*, requires fast-flowing, cold mountain streams and lakes with ample crustaceans and insect larvae (Nowak and Paradiso, 1983; Palmeirim and Hoffmann, 1983). *Galemys pyrenaicus* will seek shelter in the crevices

between large rocks or small caves along the banks of rivers or take over the burrows of other animals, but *Galamys* rarely digs its own burrow (Palmeirim and Hoffmann, 1983). *Desmana moschata* will make nests on the shoreline under vegetation and roots above the high waterline, and all entrances to their nests are only accessible underwater (Palmeirim and Hoffmann, 1983; MacDonald, 1984). Both species occupy relatively shallow (0.5-2 m in depth), rocky-bottom water with ample spaces for invertebrates to hind (Palmeirim and Hoffmann, 1983).

Having a Desmanini-like talpid at the Gray Fossil Site suggests that parts of the paleosinkhole lake could have had permanent, year-round water that might have sustained year-round aquatic invertebrate populations. This is supported by the presence of fossil fish, neotenic salamanders, and beaver material at the site (Parmalee et al., 2002; Boardman and Schubert, 2011; Mead et al., 2012; Bourque and Schubert, 2015; Jasinski, 2018). If the fossil desman was behaviorally analogous with modern desmans, it would suggest that some parts of the paleosinkhole lake would likely have been relatively shallow (< 2 m in depth), as that is optimal foraging depth for extant desmans. Excavations clearly show the bottom of the lake would have been somewhat rocky with soft sediment for invertebrates to hide in. The edges of the lake could have had some rocks, a lot of low vegetation, or a combination of the two. The GFS desman likely would have nested close to the water's edge in either the thick vegetation or in void space between large enough rocks. The water at the edge of the lake would have been calm enough for fine sedimentation to take place and preserve microfossils, so it is unlikely that the desman material found here would be behaviorally analogous with *Galemys* or *Desmana*.

***Parascalops*.** Extant *Parascalops breweri* is a truly fossorial mole, spending most, if not all, of its life underground; however, it will venture to the surface to move to a new area and to drink water. The extant species occupies a variety of rocky, gravelly, and sandy soils with deposits of interspersed clay in a variety of habitats ranging from large open fields to heavily wooded areas (Hallett, 1978). *Parascalops breweri* is not known to permanently occupy places where the soil was very wet, areas where the soil had a heavy clay content, or areas on the summits of hills or ridges where the soil was hard, dry, sandy and without the protection of trees or shrubs (Eadie, 1939). They are known to eat just about any subterranean invertebrate that they come across while hunting in their tunnels (Eadie, 1939; Hallett, 1978).

The Gray Fossil Site *Parascalops grayensis* sp. nov. is morphologically similar to, and found within the extant range of, the extant species and was similarly classified as fossorial by the canonical variates analysis. We have no definitive way of knowing how extinct animals behaved, but we can hypothesize an animal's ecology based on extant animal behavior, functional morphology, and localized paleoenvironments. Therefore, based on extant *Parascalops* behavior as well as lithological, floral, and pollen analyses of the Gray Fossil Site, this suggests that GFS *Parascalops* was likely an exclusive burrower, and possibly burrowing in soil away from the lake's edge in wooded areas, as this is where the ideal soil and food sources are for the extant species.

***Mioscalops*.** Currently, there are no known extant relatives of this genus, but this is because we do not know how this taxon is related to any extant taxa. Based on the results of the hierarchical cluster analysis, *Mioscalops* is most morphologically similar to *Condylura cristata* and *Scapanulus oweni*, although *S. oweni* bears the greatest morphological resemblance. Thus, *Mioscalops* may have occupied a similar ecological niche to these taxa.

Condylura cristata is a semi-fossorial and semi-aquatic talpid native to the eastern United States distributed as far north as Newfoundland and as far south as the Georgia-Florida boundary (Hamilton, 1931; Petersen and Yates, 1980). *Condylura cristata* is found in a variety of habitats, so long at the soil is moist. This species prefers to occupy areas of poor drainage, including both coniferous and deciduous forests, clearings, wet meadows, marshes, and peatlands (Hamilton, 1931; Kurta, 1995). *Condylura cristata* has also been found in the banks of streams, lakes, and ponds (Hamilton, 1931).

Scapanulus oweni is a semi-fossorial talpid endemic to China, in the provinces of Shaanxi, Gansu, Sichuan, Qinghai, and Hubei. This species is commonly found occupying the mossy undergrowth of montane fir forest (Smith and Xie, 2008). Smith and Xie (2008) described *Scapanulus oweni* as being ecologically similar to *Scaptonyx fusicaudus* (long-tailed mole) as they overlap biogeographically and environmentally. Little is known about the ecology of *Scapanulus*, but it has been suggested that it digs and maintains tunnels, like most fossorial moles, for food and shelter (Smith and Xie, 2008).

Mioscalops is morphologically distinct from all living talpid taxa and its closest living relative is currently unknown, so inferring how GFS *Mioscalops* would have behaved here is dependent on ecomorphology. The canonical variates analysis classified GFS *Mioscalops* as both fossorial and semi-fossorial. This suggests that GFS *Mioscalops* could have been a successful burrower, but also may have been able to swim or move above ground with greater ease than most highly fossorial taxa. The hierarchical cluster analysis grouped GFS *Mioscalops* more closely with *Scapanulus oweni* and *Condylura cristata*, which further supports a more generalized locomotor ecological classification for this taxon.

***Neurotrichus*.** Extant shrew moles are distinct from other moles. Their humeral morphology allows them to move above and below ground with little effort. Shrew moles are often mistaken for shrews as they bear striking resemblances, physically and ecologically, to one another. Some shrew moles (particularly *Neurotrichus*) are adept climbers, and will often climb into small bushes in search of food or a new nesting place (Dalquest and Orcutt, 1942). Shrew moles are also great swimmers and use all four of their limbs plus their tail to move in the water (Carraway and Verts, 1991; Abe et al., 2005). Shrew moles maintain burrows for nesting and hunting, but they are far less complex than fossorial talpid burrows and often have open entrances that are easy to find (Dalquest and Orcutt, 1942; Carraway and Verts, 1991; Abe et al., 2005). Shrew moles often prefer soft soils that are very easy to dig in with plenty of organic matter. Shrew moles tend to be found in temperate rainforests, where the soil is soft and deep (Dalquest and Orcutt, 1942; Ishii, 1993), although some have been found in moist, weedy/brushy areas (Dalquest and Orcutt, 1942).

The canonical variate analysis classified GFS *Neurotrichus* sp. as being semi-fossorial like most other extant shrew moles. This means that GFS *Neurotrichus* sp. could have been a soft soil digger like extant shrew moles, but it may have also been able to climb small bushes to hunt or nest, and swim more efficiently than more specialized burrowers. The hierarchical cluster analysis grouped GFS *Neurotrichus* sp. with the other extant shrew moles, specifically *Dymecodon pilirostris*, suggesting it is most morphologically similar to the extant shrew moles. If GFS *Neurotrichus* sp. maintained burrows, they would probably be close to the paleosinkhole lake's edge because there would be softer and moister soil closer to the water.

Biogeography

Historically, North America and Europe have had the highest diversity of talpids through geologic time (Gunnell et al., 2008). Peak global taxonomic diversity and biogeographical distributions occurred during the middle Miocene (Hutchison, 1968; Gorman and Stone, 1990; Gunnell et al., 2008). The GFS is unique because it has high talpid diversity, both in terms of the number of taxa present but also ecologically, at a point in geologic time when talpid diversity was on the decline worldwide. The number and ecological diversity of talpid taxa found at the GFS was unexpected; however, taxonomic occurrences of extant genera were expected because similar patterns are evident at other Blancan-aged sites (Gunnell et al., 2008).

GFS *Parascalops grayensis* sp. nov. is within the extant range of the living species (Eadie, 1939). This means that *P. grayensis* sp. nov. was occupying the same parts of the United States approximately 5 million years ago because the eastern United States has historically been forested throughout the Cenozoic (Wolfe, 1975; Guo, 1999; Graham, 1999). The genus was widespread during the early Pliocene - Pleistocene (Figure 14), getting as far north as New England in North America. The extant species, *Parascalops breweri*, is only known from North America, but a fossil species, *P. fossilis*, has been found in Europe (Skoczeń, 1993).

Mioscalops was spatially and temporally widespread in comparison to other talpid taxa. Its more generalized humerus morphology may have allowed it to occupy available niche spaces in more places than specialized taxa; therefore, finding *Mioscalops* at the Gray Fossil Site was not surprising. What is unusual is the lack of other *Mioscalops* occurrences that have been noted in the southeastern United States. Part of this is due to the lack of fossil sites being found in this part of the United States, but also because researchers have not identified their talpid material past the family level (Gunnell et al., 2008).

GFS *Neurotrichus* is the earliest record of the genus, and occurs well outside the range of the extant shrew mole *N. gibbsii*, which inhabits the west coast of North America from California to British Columbia (Carraway and Verts, 1991). Other early records of Neurotrichini include records of *Quyania* from the late Miocene of Asia and Plio-Pleistocene of Europe (Figure 14). The cluster analysis results grouped the GFS shrew mole with *Quyania europaea* and it shows morphological similarity to *Quyania* and *Neurotrichus*. Similarity of

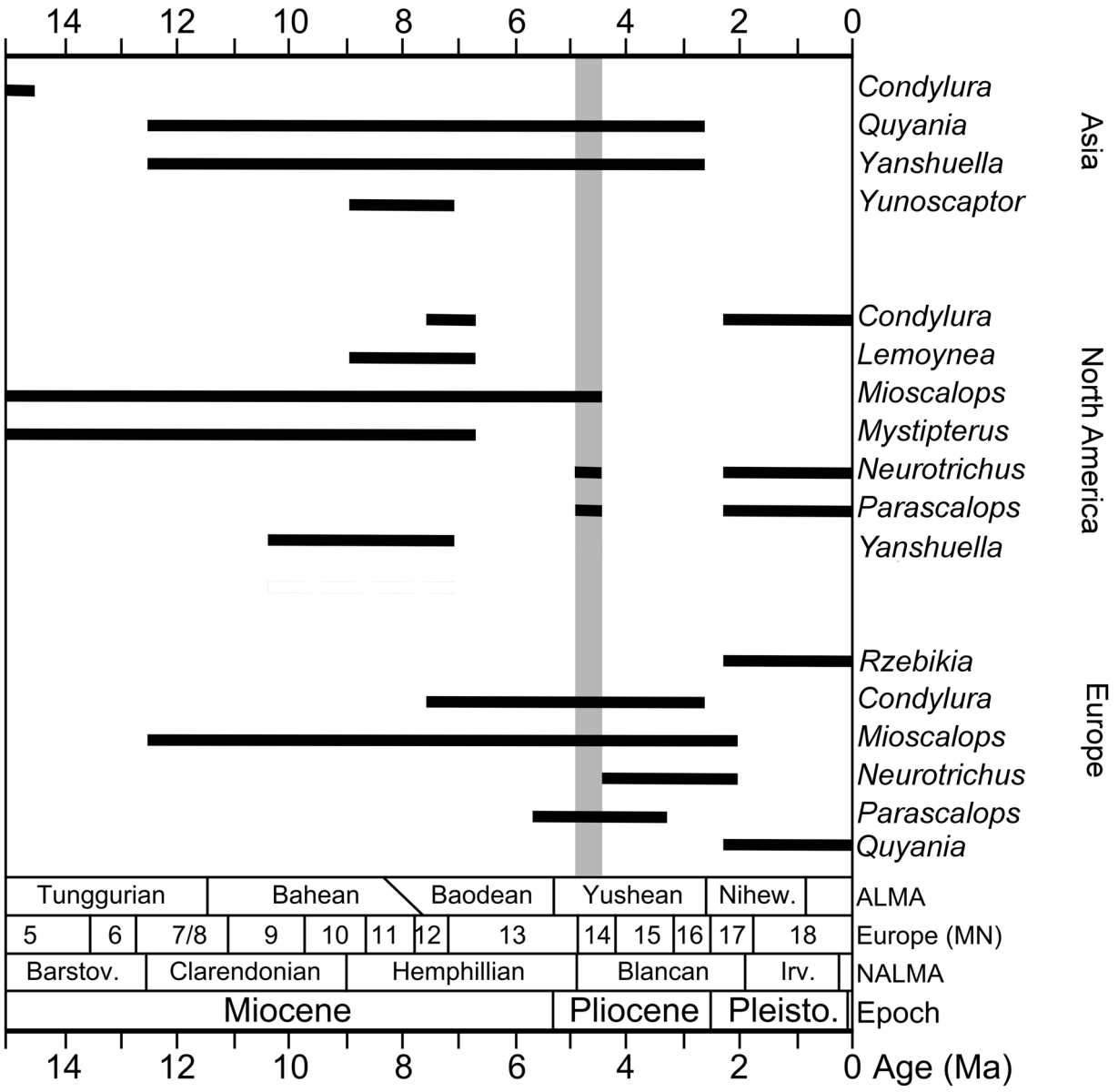

FIGURE 14. Biostratigraphic ranges of GFS taxa and morphologically similar talpids. Age of the Gray Fossil Site in gray. ALMA = Asian Land Mammal Ages, Europe MN = European Mammal Neogene zones, and NALMA = North American Land Mammal Ages.

the GFS *Neurotrichus* to the extant *N. gibbsii* and earlier neurotrichine records in Eurasia suggest there likely was a dispersal of shrew moles to North America in the late Miocene or earliest Pliocene, a time when many other taxa immigrated to the continent from Asia.

The extant tribe, Desmanini, currently has two living members, *Galemys pyrenaicus* and *Desmana moschata*. Both taxa are found exclusively in Eurasia. Fossil desmanine talpids have been found all over Eurasia throughout the Oligo-Miocene, with peak diversity during the Pliocene of Europe, but a few taxa have been found in North America. One taxon is *Lemoynea*, which was found in the late Miocene of Nebraska (Bown, 1980). Since this discovery, no other true desmanine taxa have been found in North America. Many taxa were once called Desmanini, but they all lack the synapomorphies that make them true desmans. The GFS Desmanini? (*Magnatalpa fumamons*) material

likely represents a stem desman outside the crown clade, but related to the evolutionary lineage leading to extant desmans.

The talpid occurrences at the Gray Fossil Site are quite unique. They represent first or oldest occurrences of mostly Eurasian taxa. Which raises the question of when and how did they get here? Numerous works (Sher, 1999; Flynn et al., 2003; Qiu, 2003; Woodburne, 2004; Vila et al., 2011; Guo et al., 2012; Konidaris et al., 2014) have shown that the Beringia Landbridge was open during the Mio-Pliocene and was actively used by taxa to move between the New and Old Worlds. It is likely that talpids were also using this pathway to move from Eurasia to and from North America. Particular tribes, like the Condylurini and the Scalopini, are known to originate in North America, but fossil forms are found in Europe, thus indicating that these taxa had to get from North America to Europe after the Oligocene, but before the middle Pliocene in order for the timing of their occurrence in Eurasia.

Even though the fossil record supports interchange between Eurasia and North America, western North America and Canada are lacking in fossil talpid diversity. The most likely interchange route taken by ancient talpids passed through the northern United States and Canada, but Pleistocene glaciation wiped out the fossil record. As the talpids moved into North America, they travelled west to east across Canada through the Miocene, slowly moving south into the United States as temperature began to decrease. It is unlikely that ancient talpids crossed west to east through the central United States due to presence of the Rocky Mountains creating a natural land barrier. This dispersal route is also supported by the presence of *Arctomeles* at both the Gray Fossil Site (Wallace and Wang, 2004) and the high arctic of Canada (Tedford and Harington, 2003), but not in the western part of North America.

Canonical Variate Analysis

The CVA correctly classified locomotor groups in 99.2% of original grouped cases and 95.5% when cross-validated. This means that the analysis was successfully able to correctly classify taxa with known locomotor ecologies.

Over half (n=17) of the fossil taxa were classified as semi-fossorial. The semi-fossorial locomotor ecology is the broadest ecological category included in this analysis, which includes any talpid species that is not an ecological specialist (e.g., fully fossorial, fully terrestrial, or semi-aquatic). Being such a broad ecological category, there is a lot of morphological variation being represented by this group. Most of the fossil taxa were classified as semi-fossorial because it encompasses the greatest amount of the shape variation, thus the analysis has an easier time grouping taxa into this category using the shape data (principle warps and uniform components).

There were a few fossil taxa that classified as semi-aquatic (n = 1) and terrestrial (n = 2). The single taxon that classified as semi-aquatic was *Mygalea magna*, an early Miocene-aged (early Hemingfordian NALMA, MN 3 ELMA) desman from the Czech Republic (Van den Hoek Ostende and Fejfar, 2006). The two taxa that classified as terrestrial are *Desmanella gudrunae*, an early Miocene-aged (early Hemingfordian, MN 3) uropsiline shrew mole from the Czech Republic (Van den Hoek Ostende and Fejfar, 2006), and *Gaillardia thompsoni*, a late Miocene-aged (latest Hemphillian) desman from Oregon, New Mexico, and Nebraska (Martin, 2017). *Mygalea magna* was classified as semi-aquatic, but its position in morphospace is closer to the semi-fossorial ecological group. Both *Desmanella gudrunae* and *Gaillardia thompsoni* classified as terrestrial, but *G. thompsoni* is positioned more closely to the semi-fossorial ecological group. All three of these taxa were well outside the morphospace of the group they were classified to. This suggests that these taxa might possibly have been proficient in a few different locomotor ecologies, or we do not have enough data in this analysis for it to effectively classify some taxa.

The GFS taxa all had relatively low conditional probabilities, but high posterior probabilities. This indicates that the GFS taxa were most similar to the centroid for a particular locomotor ecology (high posterior probability) but fall outside the range of variation in the training data set (low conditional probability). The GFS specimens may appear morphologically similar to extant taxa with known locomotor ecologies, but the cluster analysis results suggest that the GFS taxa may have moved and behaved differently from extant analogous forms. Even though the GFS *Neurotrichus* was classified as semi-fossorial, GFS *Mioscalops* sp. classified as both semi-fossorial and fossorial, and GFS *Parascalops grayensis* sp. nov. classified as fossorial; these taxa were probably not behaving exactly like extant taxa. It is possible that the GFS taxa represent some of the most specialized talpid taxa during the Mio-Pliocene, as we do not have a strong fossil record for talpid locomotor ecological specialization during this time period, but in

comparison to extant specialized taxa, they appear less ecologically specialized. This hypothesis is supported by the intermediate positions for the GFS taxa in morphospace.

Hierarchical Cluster Analysis

In contrast to morphological phylogenetic cladograms, both the individuals' and average position trees represent phenograms that represent morphological similarity, but also take ecological convergence into consideration. Geometric morphometrics were used to capture overall shape variation in taxa and examine how morphology reflected ecology. Variables identified as characteristics of ecology in the CVA were removed to limit some of the convergent ecological signal notorious for creating most of the problems in traditional morphological phylogenetics of talpids.

For the most part, the cluster analysis effectively removed the influence of locomotor convergence (Figures 12 and 13). There are four distinct clusters (Condylurini, shrew moles, Scalopini, and Talpini), with two more groups (Desmanini and Uropsilinae) lumped into the outgroup (Soricidae). Each group created by the cluster analysis contains the taxa originally hypothesized to be a part of that group. Also, every taxon's position in the cluster analysis can be explained and justified using traditional systematics. What this means is that humerus morphology can be used to evaluate the evolutionary relationships at the family level once ecological convergence is partially removed from an analysis.

The Gray Fossil Site taxa clustered into three different groups (Figure 13) representing three distinctly different locomotor ecologies. Each of the GFS taxa was placed into clusters with extant and other fossil taxa that share the most morphological similarities. GFS *Parascalops grayensis* sp. nov. clustered with all individuals in the genus *Parascalops*, which includes extant *P. breweri* and *P. fossilis*, along with *Proscapanus sansansiensis*. Having all the *Parascalops* individuals cluster together means that there were enough morphological similarities between the extant individuals, other fossil individuals, and the GFS samples for them to be grouped together. The combination of the GFS *P. grayensis* sp. nov., extant *P. breweri*, *Proscapanus sansansiensis*, and the other highly fossorial North American taxa (*Scapanus latimanus*, *Scapanus orarius*, *Scapanus townsedii*, *Scalopus aquaticus*, *Scaptochirus moschatua*, and *Mioscalops* sp. A) make up the Scalopini cluster. This cluster is very similar to the molecular phylogeny generated by He et al. (2016) with the exceptions of *Scapanulus oweni*, which was placed into the Condylurini cluster, being excluded and *Scaptochirus moschatua* being included. Morphologically and ecologically, this grouping makes sense. All of the taxa included in this Scalopini cluster are highly fossorial specialists, while *Scapanulus* is considered to be more semi-fossorial. *Scapanulus* morphology is most similar to that of *Condylura*, so it is not surprising that they would cluster together.

GFS *Neurotrichus* clustered with *Quyania europaea* and extant *Dymecodon pilirostris*. Interestingly, both GFS *Neurotrichus* and *Q. europaea* did not cluster with either of the other species of *Quyania*, *Neurotrichus*, or *Rzebikia*. The other species of *Quyania* (*Q. chowi*) clustered with *Rzebikia polonica* and *Neurotrichus gibbsii*; however, the *Neurotrichus* cluster is depicted as being the sister group to the *Q. europaea* cluster. This is interesting because it implies that the *Neurotrichus* lineage may have diverged much earlier than previously thought (Storch and Qui, 1983) in comparison to *Quyania*, *Urotrichus*, or *Dymecodon*. Morphologically, all of these taxa have relatively gracile humeri with minimal adaptations for fossorial life. From an ecological perspective, these taxa are semi-fossorial generalists capable of burrowing, swimming, or walking above ground with ease. It makes sense morphologically and ecologically that all of these taxa would be grouped together. Also, this general grouping matches the He et al. (2016) phylogeny.

GFS *Mioscalops* clustered with *Mioscalops* sp. E, *Yunoscaptor scalprum*, *Yanshuella*, *Scapanulus oweni*, *Mioscalops ripafodiator*, *Condylura kowalskii*, and *Condylura cristata*, which make up the Condylurini cluster. Interestingly, the cluster analysis grouped GFS *Mioscalops* more closely with *Yunoscaptor scalprum* and *Mioscalops* sp. E, implying that there is a closer relationship between these taxa. There was also distinct separation between *Yunoscaptor* and *Yanshuella*, and the placement of *Mioscalops ripafodiator* was quite surprising. Previous studies (Storch and Qui, 1983, 1991) have suggested that *Yunoscaptor* and *Yanshuella* were more closely related because most species within each genus existed in similar places at the same time, so having them separate in this cluster analysis was unexpected; however, a single species of *Yanshuella* has been found in North America, *Y. columbiana*, and it is morphological similar to *Neurotrichus gibbsii* (Hutchison, 1968; Storch and Qui, 1983; Carraway and Verts, 1991; Gunnell et al., 2008), *Condylura cristata*, and *Scapanulus oweni*. *Mioscalops ripafodiator* has been

described as being relatively specialized for a generalist taxon (Hutchison, 1968). It did not group with any of the other four taxa included in this analysis that share the same genus. One reason why these taxa could be separated is due to the lack of intraspecific variation in each genus, but it could also be due to incorrect classification. There were enough morphological distinctions between these *Mioscalops* taxa that the cluster analysis determined them to be separate. Morphologically, all of the taxa classified in the Condylurini cluster have longer and less robust humeri compared to the more fossorial specialists, though these humeri are not nearly as gracile as those of the shrew mole cluster. Condylurine talpids are still efficient burrowers, but not sufficiently adept for a completely underground lifestyle. Ecologically, the taxa included in this grouping were semi-fossorial generalist talpids that could have been good at swimming but were likely not adept at walking above ground.

The positions of the clusters generated in this analysis are relatively similar to those in the He et al. (2016) phylogeny. On the He et al. (2016) cladogram, the Uropsilinae is the most ancestral cluster, followed by the Scalopini, then the shrew mole clusters, and finally the Condylurini, Desmanini, and Talpini clusters. Condylurini and Desmanini are drawn as sister clusters and the Talpini tribe as the sister cluster to them.

In this cluster analysis, two of the six clusters (Uropsilinae and Desmanini) are nested in the outgroup. The Scalopini tribe is the first totally separate cluster and was drawn as the most ancestral clusters with the Talpini tribe nested within it. The He et al. (2016) phylogeny shows the best separation between these two clusters; however, there is weak statistical confidence supporting the position for the tribe Talpini. In this cluster analysis, there were not enough landmark differences and individuals to separate these groups; although, most of the species belonging to each tribe did cluster together. Finally, the shrew mole cluster and Condylurini cluster are depicted as being sister clusters to each other, with a shared ancestor linking them to the Scalopini group.

Even though we applied an ecological correction to the data before performing the hierarchical cluster analysis, there was still a strong ecological signal influencing the clusters. One reason why there could still be so much ecological influence is because of the evolutionary history of talpid humerus specialization. Locomotor specialization is likely what drove the change in humerus shape, thus the entire structure exists because of the evolutionary selective forces driving the shape of the humerus.

A minor issue with this hierarchical cluster analysis is the lack of intraspecific variation due to small sample sizes. In the individuals' phenogram, a single individual represents several entire clusters, such as in the Urotrichini and Uropsilinae. Also, a limited number of characters does not give the analysis enough points of reference to find similarities or differences between humerus shapes, thus creating less informed clusters. To effectively separate all taxa and resolve polytomies, there needs to be more characters (number of landmarks) than taxa. A prime example of this is the outgroup for both the individuals' and species mean phenograms (Figure 12 and 13). *Uropsilus*, *Galemys*, and *Gaillardia* were grouped with Soricidae (true shrews). Morphologically, all of these taxa are relatively similar looking with elongated humeral shafts and reduced proximal ends, thus the cluster analysis grouped them together. Molecular data shows these taxa are more distantly related to one another (He et al., 2016), but small sample sizes, limited character sampling, and similar morphology is causing these taxa to be grouped together.

Although convergence and limited character sampling have negatively affected the resolution of the hierarchical cluster analysis, it worked fairly well and allows new interpretations to be made about the history of the family.

CONCLUSIONS

The Gray Fossil Site has a new fossil talpid assemblage unlike any seen in North America before. There are at least four talpid taxa present at the site, and they represent four distinct locomotor ecologies each requiring a different niche space. GFS *Parascalops grayensis* sp. nov. is a typical fossorial talpid and morphologically similar to the extant species making this the oldest occurrence of the genus globally. GFS *Mioscalops* is a semi-fossorial talpid found in both Europe and North America, but this is the first occurrence in the southeastern United States. The GFS *Neurotrichus* is a semi-fossorial shrew mole, representing the earliest record of shrew mole lineage in the continent and suggests a late Miocene or earliest Pliocene dispersal of the clade to North America. The tribe Desmanini is well known from the fossil record of Eurasia, but very few specimens have been found in North America. The GFS specimens rep-

resent a new stem desman and are the first of their kind found in North America.

Geometric morphometric analyses showed that humerus shape is highly reflective of locomotor ecology in extant and fossil talpids. Through hierarchical cluster analysis, that data was also used to secondarily verify taxonomic designations for the GFS taxa. Even though convergence and limited sampling of variables affected how well the morphological cluster analysis was able perform, it did largely recreate the relationships found in the most recent molecular cladogram (He et al., 2016). All six tribes were represented on the cluster analysis phenograms, all of the shrew moles (Scaptonychini, Urotrichini, and Neurotrichini) clustered together, and there was some separation between the tribes Talpini and Scalopini. Additionally, the cluster analysis provides new information about the placement of fossil taxa and which parts of the tree still need better resolution.

ACKNOWLEDGMENTS

We would like to thank S. Haugrud and the dedicated group of volunteers that excavated and picked through thousands of pounds of sediment to find this material, A. Nye for cataloguing and housing all this material in ETMNH collections, and K. Bredehoeft for repairing all damaged fossils. We would also like to thank the following individuals for facilitating collections access: B. Compton (ETSU modern mammal collection), Los Angeles County Museum of Natural History and the Smithsonian Museum of Natural History for allowing us access to their modern mammal collections. We would also like to thank the D. Sundquist Center for Excellence in Paleontology and the National Science Foundation for their financial support of the Gray Fossil Site.

REFERENCES

Abe, H., Ishii, N., Ito, T., Kaneko, Y., Maeda, K., Miura, S., and Yoneda, M. 2005. A Guide to the Mammals of Japan First Edition. Tokai University Press, Japan.

Baird, S.F. 1858. Reports of explorations and surveys, to ascertain the most practical and economical route for a railroad from the Mississippi River to the Pacific Ocean. Beverley Tucker Printer, Washington D.C. https://doi.org/10.5962/bhl.title.139743

Bannikova, A.A., Zemlemerova, E.D., Lebedev, V.S., Aleksandrov, D.Y., Fang, Y., and Sheftel, B.I. 2015. Phylogenetic position of the Gansu mole *Scapanulus oweni* Thomas, 1912 and the relationships between strictly fossorial tribes of the family Talpidae. Doklady Biological Science, 464:230-234. https://doi.org/10.1134/S0012496615050038

Boardman, G.S. and Schubert, B.W. 2011. First Mio-Pliocene salamander fossil assemblage from the southern Appalachians. Palaeontologia Electronica, 14(2):1-19. https://palaeo-electronica.org/2011_2/257/index.html

Bourque, J.R. and Schubert, B.W. 2015. Fossil musk turtles (Kinosternidae, *Sternotherus*) from the late Miocene-early Pliocene (Hemphillian) of Tennessee and Florida. Journal of Vertebrate Paleontology, 35:e885441. https://doi.org/10.1080/02724634.2014.885441

Bown, T.M. 1980. The fossil Insectivora of Lemoyne Quarry (Ash Hollow Formation, Hemphillian), Keith County, Nebraska. Transactions of the Nebraska Academy of Sciences and Affiliated Societies, 284(13):99-122. https://digitalcommons.unl.edu/tnas/284

Brandon, S. 2013. Discovery of bald cypress fossil leaves at the Gray Fossil Site, Tennessee and their ecological significance. Unpublished undergraduate honors thesis, East Tennessee State University, Johnson City, Tennessee, USA.

Cabria, M.T., Rubines, J., Gomez-Moliner, B., and Zardoya, R. 2006. On the phylogenetic position of a rare Iberian endemic mammal, the Pyrenean desman (*Galemys pyrenaicus*). Gene, 375:1-13. https://doi.org/10.1016/j.gene.2006.01.038

Campbell, B. 1939. The shoulder anatomy of the moles. A study in phylogeny and adaptation. Developmental Dynamics, 64:1-39. https://doi.org/10.1002/aja.1000640102

Carrasco, M.A., Barnosky, A.D., Kraatz, B.P., and Davis, E.B. 2007. The Miocene mammal mapping project (MIOMAP): an online database of Arikareean through Hemphillian fossil mammals. Bulletin of the Carnegie Museum of Natural History, 39:183-188. https://doi.org/10.2992/0145-9058(2007)39[183:TMMMPM]2.0.CO;2

Carraway, L.N. and Verts, B.J. 1991. *Neurotrichus gibbsii.* Mammalian Species, 387:1-7. https://doi.org/10.2307/3504108

Czaplewski, N.J. 2017. First report of bats (Mammalia: Chiroptera) from the Gray Fossil Site (late Miocene or early Pliocene), Tennessee, USA. PeerJ, 5:e3263. https://doi.org/10.7717/peerj.3263

Dalquest, W.W. and Orcutt, D.R. 1942. The biology of the least shrew-mole, *Neurotrichus gibbsii minor.* The American Midland Naturalist, 27:387-401. https://doi.org/10.2307/2421007

DeSantis, L.R. and Wallace, S.C. 2008. Neogene forests from the Appalachians of Tennessee, USA: geochemical evidence from fossil mammal teeth. Palaeogeography, Palaeoclimatology, Palaeoecology, 266:59-68. https://doi.org/10.1016/j.palaeo.2008.03.032

Douady, C.J., Chatelier, P.I., Madsen, O., de Jong, W.W., Catzeflis, F., Springer, M.S., and Stanhope, M.J. 2002. Molecular phylogenetic evidence confirming the Eulipotyphla concept and in support of hedgehogs as the sister group to shrews. Molecular Phylogenetics and Evolution, 25:200-209. https://doi.org/10.1016/S1055-7903(02)00232-4

Doughty, E.M., Wallace, S.C., Schubert, B.W., and Lyon, L.M. 2018. First occurrence of the enigmatic peccaries *Mylohyus elmorei* and *Prosthennops serus* from the Appalachians: latest Hemphillian to Early Blancan of Gray Fossil Site, Tennessee. PeerJ, 6:e5926. https://doi.org/10.7717/peerj.5926

Eadie, W.R. 1939. A contribution to the biology of *Parascalops breweri*. Journal of Mammalogy, 20:150-173. https://doi.org/10.2307/1374372

Fischer von Waldheim, G. 1814. Zoognosia Tabulis Synopticis Illustrata. Volumen tertium, Quadrupedum reliquorum, Cetorum et Monotrymatum descriptionem continens. Typis Nicolai Sergeidis Vsevolozsky, Mosquae.

Flynn, L.J., Tedford, R.H., Novacek, M.J., Woodburne, M.O., Hunt Jr., R.M., Gould, G.C., and Adam, P.J. 2003. Vertebrate fossils and their context: contributions in honor of Richard H. Tedford. Bulletin of the American Museum of Natural History, 279:1-659.

Freeman, A. 1886. The anatomy of the shoulder and upper arm of the mole (*Talpa europaea*). Journal of Anatomy and Physiology, 20:201-219.

Gambaryan, P.P., Gasc, J.P., and Renous, S. 2002. Cinefluorographical study of the burrowing movements in the common mole, *Talpa europaea* (Lipotyphla, Talpidae). Russian Journal of Theriology, 1:91-109. https://doi.org/10.15298/rusjtheriol.01.2.03

Gong, F., Karsai, I., and Liu, Y.S.C. 2010. *Vitis* seeds (Vitaceae) from the late Neogene Gray fossil site, northeastern Tennessee, USA. Review of Palaeobotany and Palynology, 162:71-83. https://doi.org/10.1016/j.revpalbo.2010.05.005

Gorman, M.L. and Stone, R.D. 1990. The Natural History of Moles. Comstock Publishing Associates, Ithaca, New York.

Graham, A. 1999. Late Cretaceous and Cenozoic history of North American vegetation: north of Mexico. Oxford University Press, New York. https://doi.org/10.1093/oso/9780195113426.001.0001

Graham, R.W. and Lundelius Jr., E.L. 2010. Talpidae occurrence data downloaded 10 August 2017. FAUNMAP II. https://ucmp.berkeley.edu/faunmap/

Gregory, W.K. 1910. The Orders of Mammals. Part I: Typical States in the History of the Ordinal Classification of Mammals. Vol. 27. Bulletin of the American Museum of Natural History, New York. https://digitallibrary.amnh.org/handle/2246/313?show=full

Gunnell, G.F., Bown, T.M., Hutchison, J.H., and Bloch, J.I. 2008. Chapter 7: Lipotyphla, p. 89-126. In Janis, C.M., Gunnell, G.F., and Uhen, M.D. (eds.), Evolution of Tertiary Mammals of North America: Volume 2. Small mammals, xenarthrans, and marine mammals. Cambridge University Press, Cambridge, United Kingdom. https://doi.org/10.1017/CBO9780511541438

Guo, Q. 1999. Ecological comparisons between Eastern Asia and North America: historical and geographical perspectives. Journal of Biogeography, 26:199-206. https://doi.org/10.1046/j.1365-2699.1999.00290.x

Guo, P., Liu, Q., Xu, Y., Jiang, K., Hou, M., Ding, L., Pyron, R.A., and Burbrink, F.T. 2012. Out of Asia: natricine snakes support the Cenozoic Beringian dispersal hypothesis. Molecular Phylogenetics and Evolution, 63:825-833. https://doi.org/10.1016/j.ympev.2012.02.021

Hallett, J.G. 1978. *Parascalops breweri*. Mammalian Species, 98:1-4. https://doi.org/10.2307/3503954

Hamilton, W.J. 1931. Habits of the star-nosed mole, *Condylura cristata*. Journal of Mammalogy, 12:345-355. https://doi.org/10.2307/1373758

He, K., Shinohara, A., Jiang, X.L., and Campbell, K.L. 2014. Multilocus phylogeny of talpine moles (Talpini, Talpidae, Eulipotyphla) and its implications for systematics. Molecular Phylogenetics and Evolution, 70:513-521. https://doi.org/10.1016/j.ympev.2013.10.002

He, K., Shinohara, A., Helgen, K.M., Springer, M.S., Jiang, X.L., and Campbell, K.L. 2016. Talpid mole phylogeny unites shrew moles and illuminates overlooked cryptic species diversity. Molecular Biology and Evolution, 34:78-87. https://doi.org/10.1093/molbev/msw221

Hildebrand, M. 1974. Analysis of the Vertebrate Structure. First Edition. John Wiley and Sons, New York, London.

Hildebrand, M. 1985. Functional vertebrate morphology. First Edition. Belknap Press of Harvard University Press, Cambridge, Massachusetts.

Hooker, J.J. 2016. Skeletal adaptations and phylogeny of the oldest mole *Eotalpa* (Talpidae, Lipotyphla, Mammalia) from the UK Eocene: the beginning of fossoriality in moles. Palaeontology, 59:195-216. https://doi.org/10.1111/pala.12221

Hugueney, M. 1972. Les talpidés (Mammalia, Insectivora) de Coderet-Bransat (Allier) et l'évolution de cette famille au cours de l'Oligocene supérieur et du Miocene inférieur d'Europe. Documents des Laboratoires de Géologie de Lyon, 50:1-81.

Hutchison, J.H. 1968. Fossil Talpidae (Insectivora, Mammalia) from the later Tertiary of Oregon. Bulletin of the Museum of Natural History University of Oregon, 11:1-117.

Hutchison, J.H. 1974. Notes on type specimens of European Miocene Talpidae and a tentative classification of Old World Tertiary Talpidae (Insectivora: Mammalia). Geobios, 7:211-256. https://doi.org/10.1016/S0016-6995(74)80009-4

Hutchison, J.H. 1976. The Talpidae (Insectivora, Mammalia): evolution, phylogeny, and classification. Unpublished PhD Thesis, University of California Berkeley, Berkeley, California, USA.

Hutchison, J.H. 1984. Cf. *Condylura* (Mammalia: Talpidae) from the late Tertiary of Oregon. Journal of Vertebrate Paleontology, 4:600-601. https://doi.org/10.1080/02724634.1984.10012035

Hutchison, J.H. 1987. Late Pliocene (Blancan) *Scapanus* (*Scapanus*) (Talpidae: Mammalia) from the Glenns Ferry Formation of Idaho. Paleobios, 12(45):1-7.

Hutterer, R. 1995. *Archaeodesmana* Topachevski & Pashkov, the correct name for *Dibolia* Rümke, a genus of fossil water mole (Mammalia: Talpidae). Bonn Zoological Bulletin, 45:171-172.

Hutterer, R. 2005. Order Soricomorpha. p. 220-311. In Wilson, D.E. and Reeder, D.A. (eds.), Mammal Species of the World: A Taxonomic and Geographic Reference. John Hopkins University Press, Baltimore, Maryland.

IBM Corp. Released 2013. IBM SPSS Statistics for Windows, Version 25.0. IBM Corp, Armonk, New York. https://www.ibm.com/spss

Ishii, N. 1993. Size and distribution of home ranges of the Japanese shrew-mole *Urotrichus talpoides*. Journal of the Mammalogical Society of Japan, 18:87-98. https://doi.org/10.11238/jmammsocjapan.18.87

Jasinski, S.E. 2018. A new slider turtle (Testudines: Emydidae: Deirochelyinae: *Trachemys*) from the late Hemphillian (late Miocene/early Pliocene) of eastern Tennessee and the evolution of the deirochelyines. PeerJ, 6:e4338. https://doi.org/10.7717/peerj.4338

Jasinski, S.E. and Moscato, D.A. 2017. Late Hemphillian Colubrid Snakes (Serpentes, Colubridae) from the Gray Fossil Site of Northeastern Tennessee. Journal of Herpetology, 51:245-257. https://doi.org/10.1670/16-020

Klietmann, J., Nagel, D., Rummel, M., and Van den Hoek Ostende, L.W. 2015. A gap in digging: the Talpidae of Petersbuch 28 (Germany, Early Miocene). Paleaontologische Zeitschrift, 89:563-592. https://doi.org/10.1007/s12542-014-0228-2

Konidaris, G.E., Roussiakis, S.J., Theodorou, G.E., and Koufos, G.D. 2014. The Eurasian occurrence of the shovel-tusker *Konobelodon* (Mammalia, Proboscidea) as illuminated by its presence in the late Miocene of Pikermi (Greece). Journal of Vertebrate Paleontology, 34:1437-1453. https://doi.org/10.1080/02724634.2014.873622

Koyabu, D., Endo, H., Mitgutsch, C., Suwa, G., Catania, K.C., Zollikofer, C.P., and Sánchez-Villagra, M.R. 2011. Heterochrony and developmental modularity of cranial osteogenesis in lipotyphlan mammals. EvoDevo, 2(21):1-18. https://doi.org/10.1186/2041-9139-2-21

Kretzoi, M. and Kretzoi, M. (eds.). 2000. Fossilium catalogus 1: Animalia. Pars 137 – Index Generum et Subgenerum Mammalium. Backhuys Publishers, Germany.

Kurta, A. 2017. Mammals of the Great Lakes Region. Third Edition. University of Michigan Press, Michigan. https://doi.org/10.3998/mpub.9476502

Linnaeus, C. 1758. Systema naturae per regna tria naturae, secundum classes, ordines, genera, species, cum characteribus, differentiis, synonymis, locis. Typis Ioannis Thomae, Vindobonae, Vienna. https://doi.org/10.5962/bhl.title.559

Liu, Y.S.C. and Jacques, F.M. 2010. *Sinomenium macrocarpum* sp. nov. (Menispermaceae) from the Miocene-Pliocene transition of Gray, northeast Tennessee, USA. Review of Palaeobotany and Palynology, 159:112-122. https://doi.org/10.1016/j.revpalbo.2009.11.005

MacDonald, D. 1984. The Encyclopedia of Mammals. Facts on File Inc., New York.

Maddison, W.P. and Maddison, D.R. 2018. Mesquite: a modular system for evolutionary analysis. Version 3.40. http://mesquiteproject.org

Martín-Suárez, E., Bendala, N., and Freudenthal, M. 2001. *Archaeodesmana baetica*, sp. nov. (Mammalia, Insectivora, Talpidae) from the Mio-Pliocene transition of the Granada Basin, southern Spain. Journal of Vertebrate Paleontology, 21:547-554. https://doi.org/10.1671/0272-4634(2001)021[0547:ABSNMI]2.0.CO;2

Martin, J.E. 2017. A rare occurrence of the fossil water mole *Gaillardia* (Desmanini, Talpidae) from the Neogene in North America. Proceedings of the South Dakota Academy of Science, 96:94-98.

McKenna, M.C. and Bell, S.K. 1997. Classification of mammals: above the species level. Columbia University Press, New York.

Mead, J.I., Schubert, B.W., Wallace, S.C., and Swift, S.L., 2012. Helodermatid lizard from the Mio-Pliocene oak-hickory forest of Tennessee, eastern USA, and a review of monstersaurian osteoderms. Acta Palaeontologica Polonica, 57:111-121. https://doi.org/10.4202/app.2010.0083

Meier, P.S., Bickelmann, C., Scheyer, T.M., Koyabu, D., and Sánchez-Villagra, M.R., 2013. Evolution of bone compactness in extant and extinct moles (Talpidae): exploring humeral microstructure in small fossorial mammals. BMC Evolutionary Biology, 13(1):55. https://doi.org/10.1186/1471-2148-13-55

Miller, G.S. 1912. Catalogue of the mammals of western Europe (Exclusive of Russia) in the collection of the British Museum. Order of the Trustees. British Museum (Natural History), London.

Minwer-Barakat, R., García-Alix, A., Martín-Suárez, E., and Freudenthal, M., 2020. Early Pliocene Desmaninae (Mammalia, Talpidae) from southern Spain and the origin of the genus *Desmana*. Journal of Vertebrate Paleontology, 40:e1835936. https://doi.org/10.1080/02724634.2020.1835936

Motokawa, M. 2004. Phylogenetic relationships within the family Talpidae (Mammalia: Insectivora). Journal of Zoology, 263:147-157. https://doi.org/10.1017/S0952836904004972

Nowak, R.M. and Paradiso, J.L. 1983. Walker's Mammals of the World. Fourth Edition. Volume I. Johns Hopkins University Press, Baltimore.

Ochoa, D., Whitelaw, M., Liu, Y.S., and Zavada, M. 2012. Palynology from Neogene sediments at the Gray Fossil Site, Tennessee, USA: Floristic implications. Review of Palaeobotany and Palynology, 184:36-48. https://doi.org/10.1016/j.revpalbo.2012.03.006

Ochoa, D., Zavada, M.S., Liu, Y., and Farlow, J.O. 2016. Floristic implications of two contemporaneous inland upper Neogene sites in the eastern US: Pipe Creek Sinkhole, Indiana, and the Gray Fossil Site, Tennessee (USA). Palaeobiodiversity and Palaeoenvironments, 96:239-254. https://doi.org/10.1007/s12549-016-0233-4

Palmeirim, J.M. and Hoffmann, R.S. 1983. *Galemys pyrenaicus*. Mammalian Species, 207:1-5. https://doi.org/10.2307/3503939

Parmalee, P.W., Klippel, W.E., Meylan, P.A., and Holman, J.A. 2002. A Late Miocene-early Pliocene population of *Trachemys* (Testudines: Emydidae) from east Tennessee. Annals of the Carnegie Museum, 71:233-239. https://doi.org/10.5962/p.329869

Petersen, K.E. and Yates, T.L. 1980. *Condylura cristata*. Mammalian Species, 129:1-4. https://doi.org/10.2307/3503812

Piras, P., Sansalone, G., Teresi, L., Kotsakis, T., Colangelo, P., and Loy, A. 2012. Testing convergent and parallel adaptations in talpids humeral mechanical performance by means of geometric morphometrics and finite element analysis. Journal of Morphology, 273:696-711. https://doi.org/10.1002/jmor.20015

Polly, P.D. 2007. Chapter 15: Limbs in mammalian evolution, p. 245-268. In Hall, B.K. (ed.), Fins into Limbs: Evolution, Development, and Transformation. University of Chicago Press, Chicago.

Qiu, Z.X. 2003. Chapter 2: Dispersals of Neogene carnivorans between Asia and North America. Vertebrate fossils and their context. Bulletin of the American Museum of Natural History, 279:18-31.

Quirk, Z.J. and Hermsen, E.J. 2021. Neogene *Corylopsis* seeds from Eastern Tennessee. Journal of Systematics and Evolution, 59:611-621. https://doi.org/10.1111/jse.12571

Reed, C.A. 1951. Locomotion and appendicular anatomy in three soricoid insectivores. American Midland Naturalist, 45:513-671. https://doi.org/10.2307/2421996

Rohlf, F.J. 2006. TPS software series. Department of Ecology and Evolution, State University of New York, Stony Brook. http://www.sbmorphometrics.org/soft-utility.html

Rohlf, F.J. 2021. Why clusters and other patterns can seem to be found in analyses of high-dimensional data. Evolutionary Biology, 48:1-16. https://doi.org/10.1007/s11692-020-09518-6

Rohlf, F.J., Loy, A., and Corti, M. 1996. Morphometric analysis of Old World Talpidae (Mammalia, Insectivora) using partial-warp scores. Systematic Biology, 45:344-362. https://doi.org/10.1093/sysbio/45.3.344

Rümke, C.G. 1985. A review of fossil and recent Desmaninae (Talpidae, Insectivora). Unpublished PhD Thesis, Utrecht University, Utrecht, Netherlands. https://dspace.library.uu.nl/handle/1874/205786

Rzebik-Kowalska, B. 2014. Review of the Pliocene and Pleistocene Talpidae (Soricomorpha, Mammalia) of Poland. Palaeontologia Electronica, 17(2):1-26. https://doi.org/10.26879/457

Rzebik-Kowalska, B. and Rekovets, L. 2016. New data on Eulipotyphla (Insectivora, Mammalia) from the Late Miocene to the Middle Pleistocene of Ukraine. Palaeontologia Electronica, 19.1.9A:1-31. https://doi.org/10.26879/573

Samuels, J.X., Bredehoeft, K.E., and Wallace, S.C. 2018. A new species of *Gulo* from the Early Pliocene Gray Fossil Site (Eastern United States); rethinking the evolution of wolverines. PeerJ, 6:e4648. https://doi.org/10.7717/peerj.4648

Samuels, J.X. and Schap, J. 2021. Early Pliocene Leporids from the Gray Fossil Site of Tennessee. Eastern Paleontologist, 8:1-23.

Sánchez-Villagra, M.R., Menke, P.R., and Geisler, J.H. 2004. Patterns of evolutionary transformation in the humerus of moles (Talpidae, Mammalia): a character analysis. Mammal Study, 29:163-170. https://doi.org/10.3106/mammalstudy.29.163

Sánchez-Villagra, M.R., Horovitz, I., and Motokawa, M. 2006. A comprehensive morphological analysis of talpid moles (Mammalia) phylogenetic relationships. Cladistics, 22:59-88. https://doi.org/10.1111/j.1096-0031.2006.00087.x

Sansalone, G., Kotsakis, T., and Piras, P. 2015. *Talpa fossilis* or *Talpa europaea*? Using geometric morphometrics and allometric trajectories of humeral moles remains from Hungary to answer a taxonomic debate. Palaeontologia Electronica, 18(2):1-17. https://doi.org/10.26879/560

Sansalone, G., Kotsakis, T., and Piras, P. 2016. *Condylura* (Mammalia, Talpidae) reloaded: New insights about the fossil representatives of the genus. Palaeontologia Electronica, 19.3.54A:1-16. https://doi.org/10.26879/647

Sansalone, G., Colangelo, P., Kotsakis, T., Loy, A., Castiglia, R., Bannikova, A.A., Zemlemerova, E.D., and Piras, P. 2018. Influence of evolutionary allometry on rates of morphological evolution and disparity in strictly subterranean moles (Talpinae, Talpidae, Lipotyphla, Mammalia). Journal of Mammalian Evolution, 25(1):1-14. https://doi.org/10.1007/s10914-016-9370-9

Sansalone, G., Colangelo, P., Loy, A., Raia, P., Wroe, S., and Piras, P., 2019. Impact of transition to a subterranean lifestyle on morphological disparity and integration in talpid moles (Mammalia, Talpidae). BMC Evolutionary Biology, 19:179. https://doi.org/10.1186/s12862-019-1506-0

Sansalone, G., Castiglione, S., Raia, P., Archer, M., Dickson, B., Hand, S., Piras, P., Profico, A., and Wroe, S. 2020. Decoupling functional and morphological convergence, the study case of fossorial Mammalia. Frontiers in Earth Science, 8:112. https://doi.org/10.3389/feart.2020.00112

Schneider, C.A., Rasband, W.S., and Eliceiri, K.W. 2012. NIH Image to ImageJ: 25 years of image analysis. Nature methods, 9:671-675. https://doi.org/10.1038/nmeth.2089

Schreuder, A. 1940. A revision of the fossil water-moles (Desmaninae). Archives Néerlandaises de Zoologie, 4:201-333. https://doi.org/10.1163/036551640X00118

Schwermann, A.H. and Thompson, R.S. 2015. Extraordinarily preserved talpids (Mammalia, Lipotyphla) and the evolution of fossoriality. Journal of Vertebrate Paleontology, 35: e934828. https://doi.org/10.1080/02724634.2014.934828

Schwermann, A.H., He, K., Peters, B.J., Plogschties, T., and Sansalone, G. 2019. Systematics and macroevolution of extant and fossil scalopine moles (Mammalia, Talpidae). Palaeontology, 62:661-676. https://doi.org/10.1111/pala.12422

Sher, A. 1999. Traffic lights at the Beringian crossroads. Nature, 397:103. https://doi.org/10.1038/16341

Shinohara, A., Campbell, K.L., and Suzuki, H. 2003. Molecular phylogenetic relationships of moles, shrew moles, and desmans from the new and old worlds. Molecular Phylogenetics and Evolution, 27:247-258. https://doi.org/10.1016/S1055-7903(02)00416-5

Shinohara, A., Suzuki, H., Tsuchiya, K., Zhang, Y.P., Luo, J., Jiang, X.L., Wang, Y.X., and Campbell, K.L. 2004. Evolution and biogeography of talpid moles from continental East Asia and the Japanese Islands inferred from mitochondrial and nuclear gene sequences. Zoological science, 21:1177-1185. https://doi.org/10.2108/zsj.21.1177

Short, R.A., Wallace, S.C., and Emmert, L.G. 2019. A new species of *Teleoceras* (Mammalia, Rhinocerotidae) from the late Hemphillian of Tennessee. Bulletin of the Florida Museum of Natural History, 56:183-260.

Shunk, A.J., Driese, S.G., and Clark, G.M. 2006. Latest Miocene to earliest Pliocene sedimentation and climate record derived from paleosinkhole fill deposits, Gray Fossil Site, northeastern Tennessee, USA. Palaeogeography, Palaeoclimatology, Palaeoecology, 231:265-278. https://doi.org/10.1016/j.palaeo.2005.08.001

Shunk, A.J., Driese, S.G., and Dunbar, J.A. 2009. Late Tertiary paleoclimatic interpretation from lacustrine rhythmites in the Gray Fossil Site, northeastern Tennessee, USA. Journal of Paleolimnology, 42:11-24. https://doi.org/10.1007/s10933-008-9244-0

Siegert, C. and Hermsen, E.J. 2020. *Cavilignum pratchettii* gen. et sp. nov., a novel type of fossil endocarp with open locules from the Neogene Gray Fossil Site, Tennessee, USA. Review of Palaeobotany and Palynology, 275:104174. https://doi.org/10.1016/j.revpalbo.2020.104174

Skoczeń, S. 1980. Scaptonychini Van Valen, 1967, Urotrichini and Scalopini Dobson, 1883 (Insectivora, Mammalia) in the Pliocene and Pleistocene of Poland. Acta Zoologica Cracoviensia, 24:411-448.

Skoczeń, S. 1993. New records of *Parascalops*, *Neurotrichus* and *Condylura* (Talpinae, Insectivora) from the Pliocene of Poland. Acta Theriologica, 38:125-137.

Smith, A.T. and Xie, Y. 2008. A Guide to the Mammals of China. Princeton University Press, Princeton, New Jersey.

Storch, G. and Qiu, Z. 1983. The Neogene mammalian faunas of Ertemte and Harr Obo in Inner Mongolia (Nei Mongol), China. 2. Moles-Insectivora: Talpidae. Senckenbergiana lethaea, 64:89-127.

Storch, G. and Qiu, Z. 1991. Insectivores (Mammalia: Erinaceidae, Soricidae, Talpidae) from the Lufeng hominoid locality, Late Miocene of China. Geobios, 24:601-621. https://doi.org/10.1016/0016-6995(91)80025-U

Symonds, M.R. 2005. Phylogeny and life histories of the 'Insectivora': controversies and consequences. Biological Reviews, 80:93-128. https://doi.org/10.1017/S1464793104006566

Tedford, R.H. and Harington, C.R. 2003. An Arctic mammal fauna from the early Pliocene of North America. Nature, 425:388-390. https://doi.org/10.1038/nature01892

The NOW Community, 2017. New and Old Worlds Database of Fossil Mammals (NOW). Licensed under CC BY 4.0. Retrieved 10 August 2017 from https://nowdatabase.org/

The NOW Community. 2017. Talpidae occurrence data downloaded 20 February 2017. New and Old Worlds Database of Fossil Mammals (NOW). Licensed under CC BY 4.0. https://nowdatabase.org/now/database/

Topachevsky, V.O. 1962. Fossil desmans of the genus *Desmana* from Neogene and Anthropogene deposits of the European part of the USSR. Vykopni fauny Ukrainy i sumizhnykh terytorii, 1:5-90. (In Ukrainian)

True, F.W. 1894. Diagnoses of new North American mammals. Proceedings of the United Stations National Museum, 8:239-241.

van den Hoek Ostende, L.W. and Fejfar, O. 2006. Erinaceidae and Talpidae (Erinaceomorpha, Soricomorpha, Mammalia) from the Lower Miocene of Merkur-Nord (Czech Republic, MN 3). Beiträge zur Paläontologie, 30:175-203.

Vila, R., Bell, C.D., Macniven, R., Goldman-Huertas, B., Ree, R.H., Marshall, C.R., and Pierce, N.E. 2011. Phylogeny and palaeoecology of *Polyommatus* blue butterflies show Beringia was a climate-regulated gateway to the New World. Proceedings of the Royal Society of London B, 278:2737-2744. https://doi.org/10.1098/rspb.2010.2213

Wallace, S.C. and Wang, X. 2004. Two new carnivores from an unusual late Tertiary forest biota in eastern North America. Nature, 431:556-559. https://doi.org/10.1038/nature02819

Whidden, H.P. 2000. Comparative myology of moles and the phylogeny of the Talpidae (Mammalia, Lipotyphla). American Museum Novitates, 3294:1-53. http://hdl.handle.net/2246/2085

Whitelaw, J.L., Mickus, K., Whitelaw, M.J., and Nave, J. 2008. High-resolution gravity study of the Gray Fossil Site. Geophysics, 73:25-32. https://doi.org/10.1190/1.2829987

Wolfe, J.A. 1975. Some aspects of plant geography of the Northern Hemisphere during the late Cretaceous and Tertiary. Annals of the Missouri Botanical Garden, 62:264-279. https://doi.org/10.2307/2395198

Woodburne, M.O. 2004. Chapter 8. Global events and the North American mammalian biochronology, p. 315-343. In Woodburne, M.O. (ed.), Late Cretaceous and Cenozoic Mammals of North America. Columbia University Press, New York. https://doi.org/10.7312/wood13040-010

Worobiec, E., Liu, Y., and Zavada, M.S. 2013. Palaeoenvironment of late Neogene lacustrine sediments at the Gray Fossil Site, Tennessee, USA. Annales Societatis Geologorum Poloniae, 83:51-63.

Yalden, D.W. 1966. The anatomy of mole locomotion. Journal of Zoology, 149:55-64. https://doi.org/10.1111/j.1469-7998.1966.tb02983.x

Yates, T.L. 1984. Insectivores, elephant shrews, tree shrews and dermopterans, p. 117-144. In Anderson, S. and Jones, J.K., Jr. (eds.), Orders and families of recent mammals of the world. Wiley, New York.

Yates, T.L. and Moore, D.W. 1990. Speciation and evolution in the family Talpidae (Mammalia: Insectivora). Progress in Clinical and Biological Research, 335:1-22.

Ziegler, R. 2003. Moles (Talpidae) from the late Middle Miocene of South Germany. Acta Palaeontologica Polonica, 48:617-648.

Ziegler, R. 2005. Insectivores (Lipotyphla) and bats (Chiroptera) from the late Miocene of Austria. Annalen Des Naturhistorischen Museums in Wien A, 107:93-196.

Ziegler, R. 2012. Moles (Talpidae, Mammalia) from Early Oligocene karstic fissure fillings in South Germany. Geobios, 45:501-513. https://doi.org/10.1016/j.geobios.2011.11.017

Zobaa, M.K., Zavada, M.S., Whitelaw, M.J., Shunk, A.J., and Oboh-Ikuenobe, F.E. 2011. Palynology and palynofacies analyses of the Gray Fossil Site, eastern Tennessee: Their role in understanding the basin-fill history. Palaeogeography, Palaeoclimatology, Palaeoecology, 308:433-444. https://doi.org/10.1016/j.palaeo.2011.05.051